Stochastic Environmental Research and Risk Assessment (2023) 37:1–25
https://doi.org/10.1007/s00477-022-02270-7

ORIGINAL PAPER

A hybrid heuristic-driven technique to study the dynamics of savanna ecosystem

Muhammad Fawad Khan[1] · Muhammad Sulaiman[1] · Fahad Sameer Alshammari[2]

Accepted: 19 June 2022 / Published online: 26 July 2022

Abstract

Savanna fire has many types: Savanna woody, Savanna vegetation, and grassland. In this paper, Savanna vegetation is studied, characterized by low trees and high grass. It grows in hot and seasonally dry conditions. The Savanna vegetation is described by relating to the environment and climate. Savanna vegetation is considered a metastable mixture of trees and grass and is advanced to explain stability. The Savanna vegetation is modeled with first-order linear differential equations having grass, trees, and sapling (young trees) as components. Furthermore, the model is evaluated numerically by integrating the global search technique Sine-Cosine algorithm and local search technique Interior point algorithm. Comprehensive numerical experiments are conducted to analyze numerical results. To validate solution of proposed technique, Runge-Kutta order four method isolution is taken as a reference solution. The solutions are compared graphically with the results of the reference technique. Performance indicators Mean Absolute Deviation, Root Mean Squared Error, and Error in Nash-Sutcliffe Efficiency are implemented to verify consistency, and multiple independent runs are drawn. Furthermore, the scheme is evaluated through convergence graphs as well.

Keywords Ecosystem · Savanna · Environmental · Mathematical model · Sine-Cosine algorithm · Meta-Heuristics · Hybridization

Abbreviations

SCA	Sine cosine algorithm
IPA	Interior point algorithm
RK4	Runge-Kutta methods order four
ANN	Artificial neural network
SES	Savanna ecosystem
MAD	Mean absolute deviation
RMSE	Root mean squared error
ENSE	Error in nash-sutcliffe efficiency

1 Introduction

The Savanna vegetation is characterise by coverage area i.e low tree covered and high grass covered region Scholes and Archer (1997); Staver et al. (2011); February and Higgins (2010); Evans and Ehleringer (1994); Frost (1986); Gardner (2006); Russell et al. (1990); Hempson et al. (2007); Higgins et al. (2000); Jeltsch et al. (2000). The high Savanna vegetation region is found in many countries such as Africa, South America, Australia, India, and Myanmar (Burma)-Thailand. Along with the environmental components biotic and abiotic, the combination of grass and trees can be considered as Savanna ecosystem (SES) Accatino et al. (2010); Atwell et al. (1999); Losey and Vaughan (2006). The stability and functionality of the ecosystem are due to the composition of grass and trees. As per condition, the composition varies. Despite extensive investigation of considerable research, the mechanisms that determine global trends in this composition remain a source of contention. However, ecologists have noted that human intervention, grazing, soil type, climate change, fire, and competition for nutrients and space are the main possible mechanisms that determine the global patterns for the

✉ Muhammad Sulaiman
msulaiman@awkum.edu.pk

✉ Fahad Sameer Alshammari
f.alshammari@psau.edu.sa

Muhammad Fawad Khan
fawadaurang@gmail.com

[1] Department of Mathematics, Abdul Wali Khan University, Mardan 23200, Pakistan

[2] Department of Mathematics, College of Science and Humanities in Alkharj, Prince Sattam bin Abdulaziz University, Al-Kharj 11942, Saudi Arabia

composition Laio et al. (2006); Riginos (2009). In terms of human intervention, enormous regions of the Savanna are burned each year for various purposes, including building protection, field clearing for cattle, and conservation management. In many Savanna region it burns about 25–50% each year McLaren et al. (2004).

Native Americans produced the Pre-Columbian Savannas of North America, and Aboriginal burning resulted in many Savannas in Australia. Humans have probably been using fire in the Savanna for thousands of years in Africa. Because of these, some researchers question the significance of human interaction Accatino et al. (2010). Savannas are frequently used by grazing livestock because of their open structure. High grass biomass might result in significant biomass losses by feeding fires. Grazing reduces the fuel load, which lowers the frequency of fires while also influencing the spread's continuity and intensity. Grazing can degrade the soil's condition by causing erosion, and physical compaction Atwell et al. (1999).

Plant availability, soil moisture, and nutrients are essential factors, and they are thought to be the fundamental determinants of Savanna form and function Losey and Vaughan (2006). The quantity of water at a given location is determined by the amount of rainfall, the type of soil, and other elements such as the water's capacity to reach the roots. These characteristics can be challenging to quantify. Nutrients also follow a similar pattern. The soil's moisture determines the availability of nutrients. The problem is that minor changes in soil structure can result in considerable variations in plant accessible nutrients Staver and Levin (2012). Furthermore, several studies have reported that climate change is one of the most important variables affecting the Savanna ecosystem's dynamics. Savannas in various world regions are undergoing dramatic changes due to rising carbon dioxide levels. According to recent research, tree cover increases because of the carbon dioxide fertilization effect while grass cover decreases.

Experiments conducted in 2012 on the African Savanna ecosystem revealed that while other environmental parameters such as herbivores, fire, and rainfall were maintained constant for decades, woody plants increased. Carbon dioxide concentrations will rise within the next few decades, resulting in a rapid transition from savanna vegetation to woody Savanna. Recent data suggests that this is harming the lives of some wild animals; for example, cheetahs are having difficulties due to the shifting of the Savanna environment. Increased tree cover is expected to have no negative consequences. However, researchers have discovered that increasing forest cover may impact biological variety by producing water scarcity and may cause global warming. As a result, several experts have dubbed the Savanna ecosystem (SES) a survival battleground for trees and grasses. If trees or grass win the competition, we will have either all trees covers or grass covers, eliminating some biological diversity, including humans. Fortunately, although the competition is still ongoing, neither of them has to win because of external events such as fire, huge herbivores, and rainfall assisting them. All of these elements contribute to balancing the Savanna ecosystem of trees and grass Riginos (2009).

The contrasting study is reported by Scalon about nutrient demand and use between savanna and forest ecosystems Scalon et al. (2022), Limited increases in savanna carbon stocks over decades of fire suppression Zhou et al. (2022), study about primary productivity using geostationary operational environmental satellite at an oak savanna ecosystem is reported in Khan et al. (2020), The effects of Browsing and Grazing Herbivores determine changes in fertility of case study East African Savanna Coetsee et al. (2022), biophysical feedbacks model for the Earth system to investigate a fire-controlled in grassland or Savanna hysteresis of tropical forests Drüke (2022), the study of the Grasslands of the Indian Subcontinent and Terai-Duar Savanna based on transitions Over Decadal Timescales Banerjee et al. (2022), Variation in soil based study about seed bank and relationship with aboveground vegetation across microhabitats in a savanna-woodland Sanou et al. (2022), Singh study transitions of Forest-Savanna to understand resilience and adaptation of the tropical forest ecosystems using remote sensing Singh (2022), case study of Jinshajiang, Yunnan, strategy for establishing a natural reserve for protection of native savanna vegetation Du (2022), study about monitoring of Forest-Savanna Dynamics in transition Area like the Guineo-Congolian Takougoum Le Bienfaiteur (2022), changes in the fire-rainfall relationship at a woodland-savanna transition is reported in Hamilton et al. (2022) and study about burnt and unburnt habitats by large mammalian herbivores in a savanna-woodland ecosystem is reported by Nieman et al. (2021).

To extend the study of the Savanna ecosystem, we investigate the dynamics of the Savanna ecosystem using a contemporary mathematical model presented in Staver et al. (2011), which divides all plant life into three components: trees, tree saplings, grass and subjects them to biologically typical impacts such as fire, rainfall, and space competition. Carla Staver and Sally Archibald were awarded the Mercer Award for 2012 by the Ecological Society of America as a result of their efforts Staver et al. (2011). The award was given for a remarkable integration of remote sensing data analysis and the application of mathematical models to capture the vegetation dynamics. Tropical and subtropical Africa, Australia, South East Asia, and South America were all covered by the data sets Staver et al. (2011); Accatino et al. (2010).

For the solution of mathematical models, researchers have developed many analytical and numerical techniques. Numerical techniques are widely used to solve mathematical models. But the attention of researchers converges toward soft computing because of its efficiency and robustness. Many biological, chemical and physical problems are solved by soft computing. Such as, Adnan et al solve oscillatory behavior of heart Khan et al. (2020) using a novel neuroevolutionary approach, Analysis of temperature profiles Ahmad et al. (2020), Analysis of Virotherapy of Cancer Fawad Khan et al. (2022), Absorption of Carbon Dioxide (CO2) into Solutions by Khan et al. (2021), Falkner-Skan flow with stream-wise pressure Khan et al. (2021), unipolar electro-hydrodynamic pump Khan et al. (2021), for Stress Diagnosis in Humans Sharma et al. (2021), class of biological HIV infection model of latently infected cells Guerrero-Sánchez et al. (2021), postman problem based on molecular computing Wang et al. (2021) and much more are solved.

In this work, the SES model is transformed into an artificial neural network. And for solution of SES model, a neuro-soft computing technique based on the Sine-Cosine algorithm (SCA) and Interior Point Algorithm (IPA) is employed to solve the solution SES model. The dynamics of the SES model are split into five different scenarios. The scenarios are based on the following parameters:

- Variation in birth rate of saplings (β)
- Variation in death rate of saplings (μ)
- Variation in death rate of trees (v)
- Variation in sapling to tree recruitment (ω)
- Variation in initial conditions,

The rest of the paper is organized as follows: Sect.2 describes the mathematical model of the Savanna ecosystem, Sect. 3 consists of the proposed methodology for the solution of the SES model, Sect. 4 discusses the empirical results, and Sect. 5 concludes the work.

2 Description of Savanna Ecosystem Model

The model considered in this work is about the Savanna based on grass (G), saplings (S), and trees (T). The model is an extended form of the model considered by Staver et al. (2011); Accatino et al. (2010); Staver and Levin (2012). The space occupation is considered as:

$$G(t) + S(t) + T(t) = 1, \tag{1}$$

this implies that the space is occupied by either grass (G), saplings (S), or trees (T) for any time $t \geq 0$. The grass occupies all the space free from trees and saplings, which means grass grows faster than saplings and trees. The basic assumptions behind the model are:

- Trees are recruited from saplings, and saplings replace the grass.
- Grass hinders the formation of trees by delaying the recruitment of saplings.
- Trees produce saplings in proportion to the tree density and only in areas covered by grass.
- Trees and saplings die and are replaced by grass.

So, the mathematical model for the dynamic of ecosystem is:

$$\begin{aligned} \frac{dG}{dt} - \mu S - vT + \beta GT &= 0, \\ \frac{dS}{dt} - \beta GT + \omega(G)S + \mu S &= 0, \\ \frac{dT}{dt} - \omega(G)S + vT &= 0, \end{aligned} \tag{2}$$

here, $\omega(G)$ is the sapling to tree recruitment rate, β represents birth rate of saplings, μ is the death rate of saplings, and v is the death rate of trees, see Fig. 1. The model depends on parameters β, μ, and v here, the condition $\beta > v$ is considered, which implies that if tree's mortality rate increases than the sapling's birth rate, the system moves to $G = 1$. Furthermore, the condition $\mu \geq v$ is considered, explaining how often the trees succeed the saplings. The fire highly affects the birth rate of Savanna trees by decreasing the conversion of saplings into trees, and after fires, the birth rate of sapling increase gradually. This implies that the fire highly influences the recruitment of saplings to trees $\omega(G)$ compared to the death rate v of trees. The fire depends on the area covered by grass. If most areas are covered by grass, the fire possibility is high. If the cover of the trees is high, fire is rare. To analyze all these conditions, the model is solved by employing an optimization technique. In section 3, the employment of technique and solution process is discussed briefly.

3 Proposed Methodology

This section discusses the proposed scheme for the Savanna ecosystem (SES) solution. The scheme is designed by using an Artificial neural network (ANN).

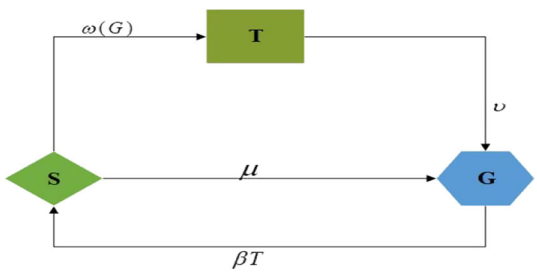

Fig. 1 Dynamics flow chart of Savanna ecosystem model

Here, the ANN-based mathematical model is designed for SES, and then for the fitness of solutions of the SES model, the fitness function is constructed using least square errors.

3.1 Mathematical model of SES

For the solution of the SES model, the feed-forward artificial neural network-based model is designed. This type of ANN is unidirectional. The layer does not form a cycle. All information moves from node to node in a single direction, as every ANN is based on an activation function. In this work, the Log-sigmoid activation function is used, given in Eq. (6), for the approximation of the solution of the SES model. The model proceeds as:

$$\left.\begin{aligned}
&\hat{G}(t) = \textstyle\sum_{i=1}^{k} a_{Gi}\theta(w_{Gi}(t) + b_{Gi}) \\
&\frac{d\hat{G}}{dt} = \sum_{i=1}^{k} a_{Gi}\theta'(w_{Gi}(t) + b_{Gi}) \\
&\frac{d^2\hat{G}}{dt^2} = \sum_{i=1}^{k} a_{Gi}\theta''(w_{Gi}(t) + b_{Gi}) \\
&\vdots \\
&\frac{d^n\hat{G}}{dt^n} = \sum_{i=1}^{k} a_{Gi}\theta^n(w_{Gi}(t) + b_{Gi})
\end{aligned}\right\}, \tag{3}$$

$$\left.\begin{aligned}
&\hat{S}(t) = \textstyle\sum_{i=1}^{k} a_{Si}\theta(w_{Si}(t) + b_{Si}) \\
&\frac{d\hat{S}}{dt} = \sum_{i=1}^{k} a_{Si}\theta'(w_{Si}(t) + b_{Si}) \\
&\frac{d^2\hat{S}}{dt^2} = \sum_{i=1}^{k} a_{Si}\theta''(w_{Si}(t) + b_{Si}) \\
&\qquad\vdots \\
&\frac{d^n\hat{S}}{dt^n} = \sum_{i=1}^{k} a_{Si}\theta^n(w_{Si}(t) + b_{Si})
\end{aligned}\right\}, \tag{4}$$

$$\left.\begin{aligned}
&\hat{T}(t) = \textstyle\sum_{i=1}^{k} a_{Ti}\theta(w_{Ti}(t) + b_{Ti}) \\
&\frac{d\hat{T}}{dt} = \sum_{i=1}^{k} a_{Ti}\theta'(w_{Ti}(t) + b_{Ti}) \\
&\frac{d^2\hat{S}}{dt^2} = \sum_{i=1}^{k} a_{Ti}\theta''(w_{Ti}(t) + b_{Ti}) \\
&\vdots \\
&\frac{d^n\hat{S}}{dt^n} = \sum_{i=1}^{k} a_{Ti}\theta^n(w_{Ti}(t) + b_{Ti})
\end{aligned}\right\}, \tag{5}$$

Eqs. (3–5) represent the artificial neural network based model of SES. Here, θ represent activation function given in Eq. (6). The ANN form of activation function and it's derivative is given in Eqs. (7) and (8) respectively.

$$\theta(t) = \frac{1}{1+e^{-t}}, \tag{6}$$

$$\hat{\theta}(t) = \sum_{i=1}^{k} a_i\left(\frac{1}{1+e^{-(w_i t+b_i)}}\right), \tag{7}$$

$$\hat{\theta}'(t) = \sum_{i=1}^{k} a_i w_i\left(\frac{e^{-(w_i t+b_i)}}{(1+e^{-(w_i t+b_i)})^2}\right). \tag{8}$$

The approximation of solution given in Eqs. (7) and (8) based on variables known as weights, represented by set W, where $W = [\mathbf{a}_i, \mathbf{w}_i, \mathbf{b}_i]$ and it's constituents $\mathbf{a}_i = \{a_1, a_2, a_3, ...a_k\}$, $\mathbf{w}_i = \{w_1, w_2, w_3, ...w_k\}$ and $\mathbf{b}_i = \{b_1, b_2, b_3, ...b_k\}$. These weights are approximate by the proposed numerical technique. Random sets of weights are generated in a given interval. The best weights are chosen by their fitness values from generated sets of weights. The fitness function must be designed to evaluate approximated solutions based on set W.

3.2 Fitness function for SES model

The fitness function for the SES model is constructed by using mean square error. The means square error is a method used to estimate the means of the squared errors. It tells how nearer is the solution to reference solution. The fitness function is define as:

$$minimize \quad E = E_G + E_S + E_T + E_c, \tag{9}$$

in Eq. (9), E is sum of errors in model of SES and its initial conditions. The E_G is the mean square of first equation in model (2), E_S is the mean square error of second, and E_T is mean square error of third equation. Where E_c is mean square errors of initial conditions. The E_G, E_S and E_T are define as:

$$E_G = \frac{1}{N}\sum_{i=1}^{N}\left(\frac{d\hat{G}_i}{dt} - \mu\hat{S}_i - \nu\hat{T}_i + \beta\hat{G}_i\hat{T}_i\right)^2 \tag{10}$$

$$E_S = \frac{1}{N}\sum_{i=1}^{N}\left(\frac{d\hat{S}_i}{dt} - \beta\hat{G}_i\hat{T}_i + \omega(G)\hat{S}_i + \mu\hat{S}_i\right)^2 \tag{11}$$

$$E_T = \frac{1}{N}\sum_{i=1}^{N}\left(\frac{d\hat{T}_i}{dt} - \omega(G_i)\hat{S} + \nu\hat{T}_i\right)^2 \tag{12}$$

$$E_c = \frac{1}{3}\left(\left(\hat{G} - G_0\right)^2 + \left(\hat{S} - S_0\right)^2 + \left(\hat{T} - T_0\right)^2\right). \tag{13}$$

In the above equations, N is the number of input points that depend on the choice of step size. If in the interval [0, 1] the step size is chosen as 0.1, the number of input points will be 11. The selection of ANN weights is based on their fitness value, and weights with a minimum error are considered best weights. The Eq. (9) justify the quality of the solution and how much it converges to an exact or reference solution.

3.3 Optimization technique ANN-SCA-IPA

A novel hybrid optimization technique is proposed to minimize Eq. (9) and find the best-fitted set of weights for solution of the SES model. As optimization techniques are categorized as local search and global search techniques. The local search starts from an initial point is executed with a single solution, and develops by implementing neighborhood procedures, such as hill-climbing, tabu search, etc. The exploitation power is the advantage of local search techniques. In contrast, the disadvantages are that it does not focus on the exploration (global) search procedure. The global search techniques are population-based. Produce random solutions using provided population. The global search techniques focus on exploration rather than exploitation. These two search methodologies are hybridized in this work. For global search, the Sine Cosine Algorithm (SCA) is implemented, while for local search, the Interior-point algorithm (IPA) is used; a flow chart is given in Fig. 2. The Sine Cosine Algorithm was developed by Ali Jalili Mirjalili (2016). The SCA is motivated by trigonometric ratios sine and cosine. The SCA generates random solutions and then shifts to next step based on their fitness. Generally, the global search techniques start the optimization procedure with randomly generated solutions. These initial solutions are evaluated by using an objective function. This development of solutions is basis on a set of optimization operators. In SCA, the following equations are used for updating the solutions:

$$X_i^{t+1} = X_i^t + r_1 \times \sin(r_2) \times \left| r_3 P_i^t - X_i^t \right|, \tag{14}$$

$$X_i^{t+1} = X_i^t + r_1 \times \cos(r_2) \times \left| r_3 P_i^t - X_{ii}^t \right|, \tag{15}$$

in above equations X_i^t is position of current solution at t^{th} in i^{th} dimension, || is absolute operator, r_1, r_2, r_3 are random numbers, P_i is the position at i_th dimension. The Eqs. (14) and (15) combined together and implemented as:

$$X_i^{t+1} \begin{cases} X_i^t + r_1 \times \sin(r_2) \times \left| r_3 P_i^t - X_i^t \right|, & r_4 < 0.5 \\ X_i^t + r_1 \times \cos(r_2) \times \left| r_3 P_i^t - X_{ii}^t \right|, & r_4 \geq 0.5' \end{cases} \tag{16}$$

here r_4 is a random number in [0,1].

In Eq. (16) has four parameters, r_1, r_2, r_3 and r_4.The movement direction to next position is represented by r_1. The parameter r_2 denotes the movement toward the target. The parameter r_3 denotes a random weight score for the target to stochastically assert $(r_3 > 1)$ or deemphasize $(r_3 < 1)$ the influence of the target in determining the distance and fourth parameter r_4 is used for switching among trigonometric functions sine and cosine, which is given in Eq. (16). The SCA is hybridized with Interior Point Algorithm (IPA) to improve the generated solution. The IPA can be implemented for linear and non-linear optimization problems. The IPA has many advantages over Sequential quadratic programming and trust regions to solve the iterative problems Byrd et al. (1999). The exploitation procedure of IPA refines the quality of solutions. The detail pseudocode is given in Algorithm 1 while the working flow chart is given in Fig. 2.

3.4 Performance operators

To validate and evaluate the performance of proposed methodology, SCA-IPA-ANN, statistical performance operators are used. Based on Nash-Sutcliffe efficiency, the implemented performance indicators are Mean Absolute Deviation (MAD), Root Mean Squared Error (RMSE), and Error in Nash-Sutcliffe Efficiency (ENSE). For each variable in the SES model, performance operators are defined. The following mathematical formulations shows the definition of performance indicators:

$$\begin{aligned} &[\mathrm{MAD}_G \;\; \mathrm{MAD}_S \;\; \mathrm{MAD}_T] \\ &= \left[\frac{1}{\mathrm{m}} \sum_{i=1}^{\mathrm{m}} \left| G_\mathrm{i} - \hat{G}_i \right| \;\; \frac{1}{\mathrm{m}} \sum_{i=1}^{\mathrm{m}} \left| S_i - \hat{S}_i \right| \;\; \frac{1}{\mathrm{m}} \sum_{i=1}^{\mathrm{m}} \left| T_\mathrm{i} - \hat{T}_i \right| \right], \end{aligned} \tag{17}$$

$$\begin{aligned} &[\mathit{RMSE}_G \; \mathit{RMSE}_S \; \mathit{RMSE}_T], \\ &= \left[\sqrt{\frac{1}{m} \sum_{i=1}^{m} \left(G_i - \hat{G}_i \right)^2} \;\; \sqrt{\frac{1}{m} \sum_{i=1}^{m} \left(S_i - \hat{S}_i \right)^2} \;\; \sqrt{\frac{1}{m} \sum_{i=1}^{m} \left(T_i - \hat{T}_i \right)^2} \right], \end{aligned} \tag{18}$$

$$\begin{aligned} &[\mathrm{NSE_G} \; \mathrm{NSE_S} \; \mathrm{NSE_T}] \\ &= \left[1 - \frac{\sum_{i=1}^{m} \left(G_i - \hat{G}_i \right)^2}{\sum_{i=1}^{m} \left(G_i - \bar{G}_i \right)^2} \; 1 - \frac{\sum_{i=1}^{m} \left(S_i - \hat{S}_i \right)^2}{\sum_{i=1}^{m} \left(S_i - \bar{S}_i \right)^2} \; 1 - \frac{\sum_{i=1}^{m} \left(T_i - \hat{T}_i \right)^2}{\sum_{i=1}^{m} \left(T_i - \bar{T}_i \right)^2} \right], \end{aligned} \tag{19}$$

$$\begin{bmatrix} [\,\mathrm{ENSE}_G \; \mathrm{ENSE}_S \; \mathrm{ENSE}_T\,] \\ = [|1 - \mathit{NSE}_G| \quad |1 - \mathit{NSE}_S| \quad |1 - \mathit{NSE}_T|] \end{bmatrix}. \tag{20}$$

In Eqs. (17–19), m is number of input depend on the choice of step size, G, S, and T are reference solutions obtained by RK4 and $\hat{G}$, $\hat{S}$, and $\hat{T}$ are numerical solutions executed by ANN-SCA-IPA technique. The best solutions give zero value for MAD, RMSE, and ENSE. The value of ENSE depends on the value of NSE. The value of NSE is 1. As much as the value of NSE is nearer to 1, the value of ENSE moves toward 0. Which indicates the convergence of ANN-SCA-IPA technique. Furthermore, the global operators of MAD, RMSE, and ENSE are also utilized, abbreviated as GMAD, GRMSE, and GENSE. The definition of the global variant are as given:

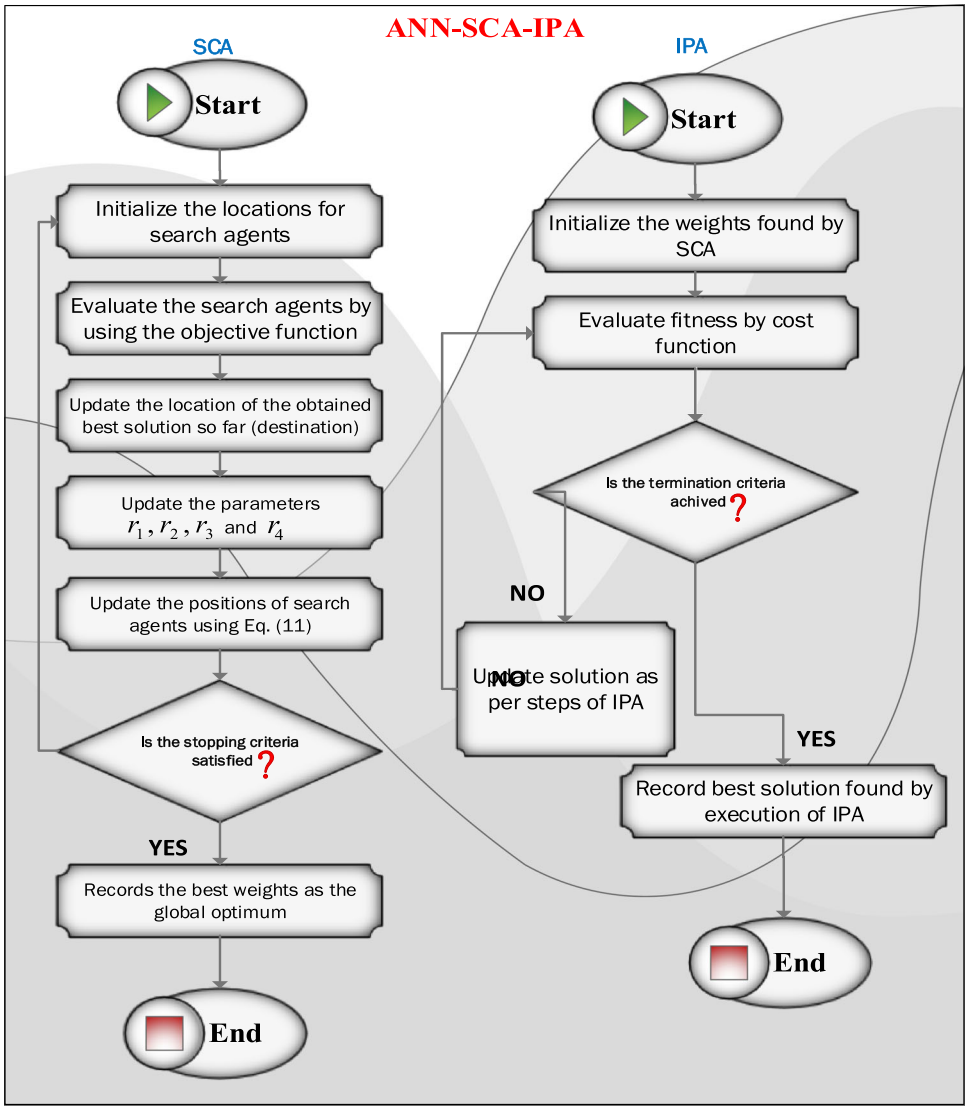

Fig. 2 The flow chart of proposed methodology ANN-SCA-IPA. Here, SCA generates number of random solutions evaluate it on its fitness, then it provides to IPA as initiail point for further refinement. The fittest weights obtain for solution of SES model

$$[\mathrm{GMAD}_G \ \mathrm{GMAD}_S \ \mathrm{GMAD}_T] = \left[\frac{1}{I}\sum_{i=1}^{I}\left(\frac{1}{m}\sum_{k=1}^{m}(|G_i-\hat{G}_i|)\right) \ \frac{1}{I}\sum_{i=1}^{I}\left(\frac{1}{m}\sum_{k=1}^{m}(|S_i-\hat{S}_i|)\right) \ \frac{1}{I}\sum_{i=1}^{I}\left(\frac{1}{m}\sum_{K=1}^{m}(|T_i-\hat{T}_i|)\right)\right], \tag{21}$$

$$[GRMSE_G GRMSE_S GRMSE_T] = \begin{bmatrix} \frac{1}{I}\sum_{i=1}^{I}\left(\sqrt{\frac{1}{m}\sum_{k=1}^{m}(G_i-\hat{G}_i)^2}\right) \\ \frac{1}{I}\sum_{i=1}^{I}\left(\sqrt{\frac{1}{m}\sum_{k=1}^{m}(S_i-\hat{S}_i)^2}\right) \\ \frac{1}{I}\sum_{i=1}^{I}\left(\sqrt{\frac{1}{m}\sum_{k=1}^{m}(T_i-\hat{T}_i)^2}\right) \end{bmatrix}, \tag{22}$$

$$[\mathrm{GENSE}_G \mathrm{GENSE}_S \mathrm{GENSE}_T] = \left[\frac{1}{I}\sum_{i=1}^{I}\left(1-\frac{\sum_{k=1}^{m}(G_i-\hat{G}_i)^2}{\sum_{k=1}^{m}(G_i-\hat{G}_i)^2}\right) \ \frac{1}{I}\sum_{i=1}^{I}\left(1-\frac{\sum_{k=1}^{m}(S_i-\hat{S}_i)^2}{\sum_{k=1}^{m}(S_i-\hat{S}_i)^2}\right) \ \frac{1}{I}\sum_{i=1}^{I}\left(1-\frac{\sum_{k=1}^{m}(T_i-\hat{T}_i)^2}{\sum_{k=1}^{m}(T_i-\hat{T}_i)^2}\right)\right]. \tag{23}$$

In Eqs. (21–23), I represent the number of execution(runs) of ANN-SCA-IPA technique. The value of GMAD, RMSE, and GENSE depends on the average value of its respective operator.

Table 1 Pseudo code of proposed hybrid soft computing technique ANN-SCA-IPA

Sine Cosine Algorithm: Start
Inputs: Appropriate population size P, Upper and Lower bound (UB LB), Max_iter. The individuals of P random Solutions $(x_i(i = 1,2,3,...,P))$ representing decision variables (weights) of ANN as:
W=[**a**,**w**,**b**]
Population: Generate population **P** with the set of **W** as:
P=$[W_1,W_2,W_3,...,W_m]^t$
a=$[a_1,a_2,a_3,...,a_m]$, **w**=$[w_1,w_2,w_3,...,w_m]$ and **b**=$[b_1,b_2,b_3,...,b_m]$
Output: The Global best weights of Sine Cosine Algorithm $W_{SCA_{Best}}$
Initializations: Formulated weights **W** and initial population **P**.
Fitness evaluation: Calculate the fitness value of each **W** in **P** and generate random solution inside the search zone (LB UB)

$$x_i\text{=best position of minimum fitness}$$
$$Solution_{random}\text{=generate random solution}$$
$$Solution_{Updated}\text{=Apply operation}\,(x_i, Solution_{random})$$
$$Solution_{Best}\text{=Apply operation}\,(Solution_{Updated}, x_{i's})$$

Termination: Stop SCA if the following termination criteria meet
'Max_iter' equal to 1000
if $(\text{fitness}(Solution_{Best}) < \text{fitness}(x_i))$
Update $x_i = Solution_{Best}$
Storage: Store $W_{SCA_{Best}}$, Fitness values, time, Function evaluations
Sine Cosine Algorithm: End
Interior Point Algorithm: Start
Inputs: $W_{SCA_{Best}}$ as starting point of interior point algorithm
Output: Weight vector of SCA-IPA i.e., $W_{SCA-IPA}$
Initialization: Start-Point as $W_{SCA-IPA}$ Assignments for iterations, bounds and other settings
Termination: Adaption process ends for any of the following conditions:
'Fitness' ϵ less than or equal to 10^{-13}
'total iterations' ϵ less than or equal to 3000
'TolFun' less than or equal to 10^{-18}
'TolX' less than or equal to 10^{-20}
'TolCon' less than or equal to 10^{-18}
'MaxFunEvals' less than or equal to 200,000
while (Terminate required achieved)
Fitness evaluation: Calculate fitness of each **W**
Fine-tuning: Use "fmincon" routine algorithm interior-point for IPA. Update parameters of **W** for each iteration of IPA and calculate fitness of modified **W**
Storage: Store weights vector $W_{SCA-IPA}$, fitness value, iterations, functions evaluations and time.
Interior Point Algorithm: End

4 Discussion and Results

This section consists of discussion and empirical results of the dynamic characteristic of the Savanna ecosystem (SES) model, given in Eq. (2). The SES model is discussed in its empirical results for different scenarios. These scenarios are based on the values of its parameters birth rate of saplings β, death rate of saplings μ, death rate of trees v and sapling to tree recruitment ω. The results are based on 100 execution (runs).

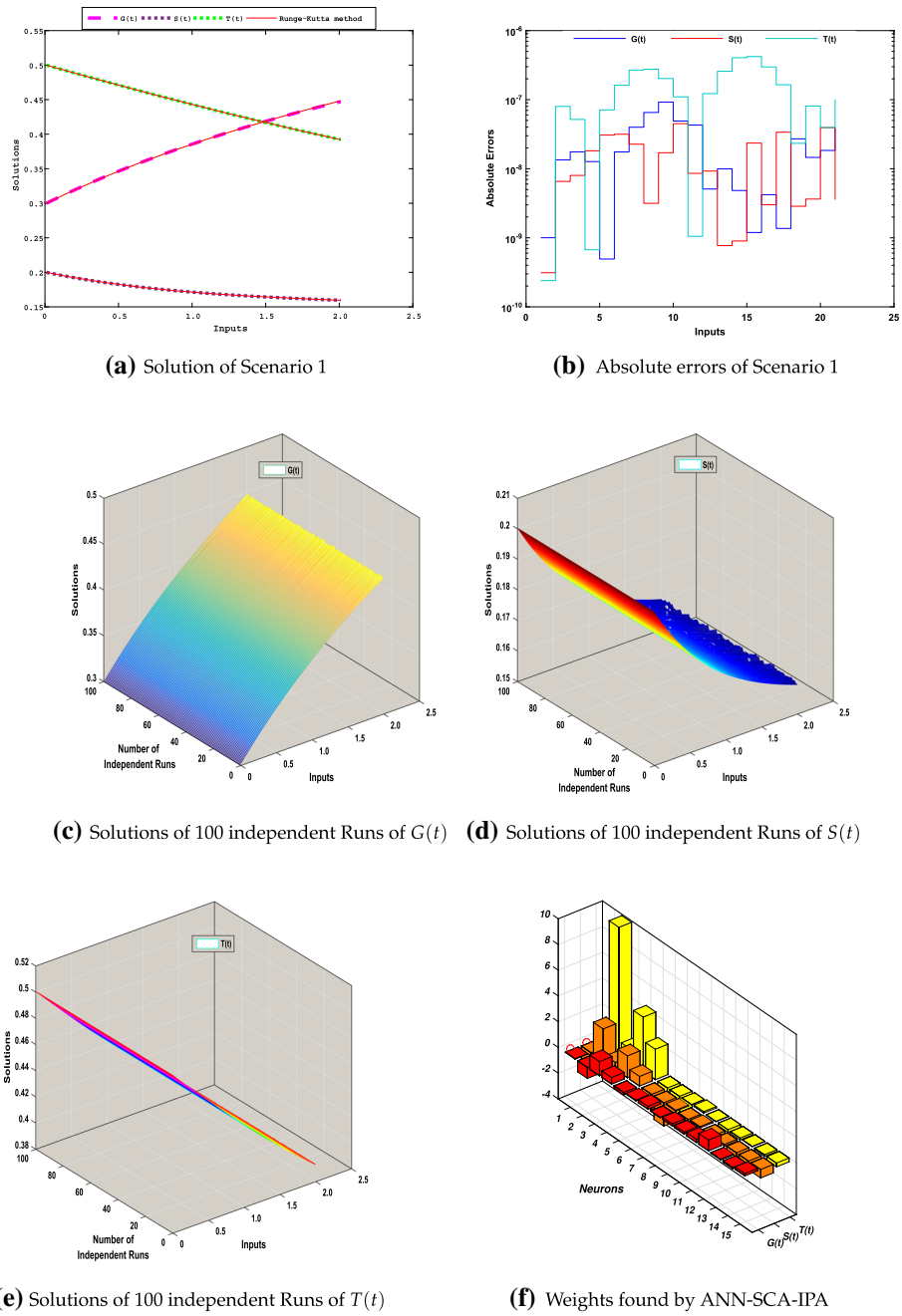

(a) Solution of Scenario 1 **(b)** Absolute errors of Scenario 1

(c) Solutions of 100 independent Runs of $G(t)$ **(d)** Solutions of 100 independent Runs of $S(t)$

(e) Solutions of 100 independent Runs of $T(t)$ **(f)** Weights found by ANN-SCA-IPA

Fig. 3 Graphical representation of Scenario 1

4.1 Scenario 1

This scenario is based on the following values, of SES model in Eq. (2), birth rate of saplings $\beta = 0.5$, death rate of sapling $\mu = 0.4$, death rate of trees $v = 0.2$ and sapling to tree recruitment $\omega = 0.2$. Multiple executions are done for the SES model to collect a large number of data. The fitness function with 10 input points can be updated as:

$$\begin{aligned} E = \frac{1}{10}&\left(\frac{dG_i}{dt} - 0.4S_i - 0.2T_i + 0.5G_iT_i\right)^2 \\ &+ \left(\frac{dS_i}{dt} - 0.5G_iT_i + 0.2S_i + 0.4S_i\right)^2 \\ &+ \left(\frac{dT_i}{dt} - 0.2S + 0.2T_i\right)^2 \\ &+ \frac{1}{3}\left((G_i - 0.3)^2 + (S_i - 0.2)^2 + (T_i - 0.5)^2\right), \end{aligned} \tag{24}$$

Table 2 Absolute errors of scenario 1 with reference solution

t	G(t)				S(t)			T(t)			
	MIN	MAX	MEAN	STD	MIN	MAX	MEAN	STD	MIN	MAX	MEAN	STD
1.0	4.91×10^{-08}	1.51×10^{-04}	2.52×10^{-06}	1.51×10^{-05}	4.50×10^{-08}	9.39×10^{-06}	1.44×10^{-06}	1.30×10^{-06}	1.10×10^{-07}	2.40×10^{-05}	1.88×10^{-06}	2.29×10^{-06}
1.1	4.29×10^{-08}	1.61×10^{-04}	2.49×10^{-06}	1.60×10^{-05}	8.57×10^{-09}	1.07×10^{-05}	1.37×10^{-06}	1.40×10^{-06}	1.05×10^{-09}	2.61×10^{-05}	1.92×10^{-06}	2.50×10^{-06}
1.2	5.09×10^{-09}	1.69×10^{-04}	2.42×10^{-06}	1.69×10^{-05}	9.25×10^{-09}	1.17×10^{-05}	1.28×10^{-06}	1.46×10^{-06}	1.22×10^{-07}	2.81×10^{-05}	1.94×10^{-06}	2.70×10^{-06}
1.3	9.94×10^{-09}	1.76×10^{-04}	2.34×10^{-06}	1.76×10^{-05}	7.71×10^{-10}	1.23×10^{-05}	1.16×10^{-06}	1.50×10^{-06}	2.58×10^{-07}	3.01×10^{-05}	1.93×10^{-06}	2.90×10^{-06}
1.4	4.84×10^{-09}	1.82×10^{-04}	2.25×10^{-06}	1.82×10^{-05}	8.99×10^{-10}	1.27×10^{-05}	1.04×10^{-06}	1.51×10^{-06}	4.05×10^{-07}	3.19×10^{-05}	1.90×10^{-06}	3.09×10^{-06}
1.5	1.19×10^{-09}	1.87×10^{-04}	2.30×10^{-06}	1.87×10^{-05}	2.35×10^{-08}	1.28×10^{-05}	9.32×10^{-07}	1.48×10^{-06}	4.21×10^{-07}	3.37×10^{-05}	1.85×10^{-06}	3.27×10^{-06}
1.6	4.21×10^{-09}	1.90×10^{-04}	2.43×10^{-06}	1.90×10^{-05}	3.01×10^{-09}	1.26×10^{-05}	8.53×10^{-07}	1.41×10^{-06}	2.98×10^{-07}	3.54×10^{-05}	1.79×10^{-06}	3.45×10^{-06}
1.7	1.37×10^{-09}	1.93×10^{-04}	2.57×10^{-06}	1.92×10^{-05}	3.38×10^{-08}	1.22×10^{-05}	7.99×10^{-07}	1.32×10^{-06}	1.65×10^{-07}	3.70×10^{-05}	1.71×10^{-06}	3.62×10^{-06}
1.8	2.71×10^{-08}	1.95×10^{-04}	2.71×10^{-06}	1.94×10^{-05}	2.86×10^{-09}	1.17×10^{-05}	7.57×10^{-07}	1.22×10^{-06}	2.33×10^{-08}	3.86×10^{-05}	1.62×10^{-06}	3.79×10^{-06}
1.9	1.46×10^{-08}	1.95×10^{-04}	2.84×10^{-06}	1.94×10^{-05}	3.64×10^{-09}	1.09×10^{-05}	7.32×10^{-07}	1.12×10^{-06}	8.08×10^{-08}	4.01×10^{-05}	1.52×10^{-06}	3.95×10^{-06}
2.0	1.84×10^{-08}	1.95×10^{-04}	2.96×10^{-06}	1.94×10^{-05}	3.94×10^{-08}	9.97×10^{-06}	7.18×10^{-07}	1.03×10^{-06}	3.95×10^{-08}	4.15×10^{-05}	1.41×10^{-06}	4.10×10^{-06}

and the associated initial conditions are $G(0) = 0.3, S(0) = 0.2$ and $T(0) = 0.5$.

The sum of mean square errors of each equation is minimized by ANN-SCA-IPA technique. The solution obtained by ANN-SCA-IPA is compared graphically with the results of Range-Kutta order (RK4) in Fig. 3(a). The RK4 is implemented using Matlab's built-in function, Ode45. Each variable is plotted for 100 independent runs in sub-figure 3(c), (d) and (e). The solutions of RK4 are taken as a reference solution. The absolute errors between reference solution and solution by ANN-SCA-IPA algorithm are also drawn in Fig. 3(b). For evaluation of fitness values, statistical terms maximum (MAX), minimum (MIN), and standard deviation (STD) are used. The data for MAX, MIN, and STD is reported in Table 2. The values of minimum for all variables are in between 10^{-07} and 10^{-09}, the values of maximum are lies in 10^{-04} and 10^{-06}, the value of mean is in 10^{-06} and 10^{-07} and the values of standard deviation lies in 10^{-05} and 10^{-06}. The weights are drawn three-dimensionally given in sub-figure 3(f). The best weights found by execution of ANN-SCA-IPA technique are used in Eq. (6) which give the solution for SES model is given as:

$$
\begin{aligned}
\hat{G}(t) &= \frac{0.027811602}{1+\mathrm{e}^{-(-1.55051289t+0.558231056)}} \\
&+ \frac{-0.854449245}{1+\mathrm{e}^{-(2.494552979t+9.892323223)}} \\
&+ \frac{1.099000774}{1+\mathrm{e}^{-(0.540789435t+1.047194101)}} \\
&+ \frac{0.512345539}{1+\mathrm{e}^{-(1.692944341t+4.210773225)}} \\
&+ \frac{-0.19878417}{1+\mathrm{e}^{-(0.747479484t+2.361581194)}}, \\
\hat{S}(t) &= \frac{0.059194892}{1+\mathrm{e}^{-(-1.218828605t-0.560106622)}} \\
&+ \frac{0.218764764}{1+\mathrm{e}^{-(-1.814152018t-2.652484)}} \\
&+ \frac{-0.003759589}{1+\mathrm{e}^{-(0.064715941t+0.013521261)}} \\
&+ \frac{0.160117491}{1+\mathrm{e}^{-(-0.185136338t+0.11001229)}} \\
&+ \frac{0.165264582}{1+\mathrm{e}^{-(0.086348852t-0.027090774)}}, \\
\hat{T}(t) &= \frac{0.256146466}{1+\mathrm{e}^{-(-0.286720253t-0.204522208)}} \\
&+ \frac{0.83903796}{1+\mathrm{e}^{-(-0.136194189t-0.143813182)}} \\
&+ \frac{-0.068517501}{1+\mathrm{e}^{-(-0.346705535t-0.021350454)}} \\
&+ \frac{-0.105794694}{1+\mathrm{e}^{-(-0.395919634t-0.131061835)}} \\
&+ \frac{0.18490423}{1+\mathrm{e}^{-(-0.658944399t-0.295242787)}},
\end{aligned}
\tag{25}
$$

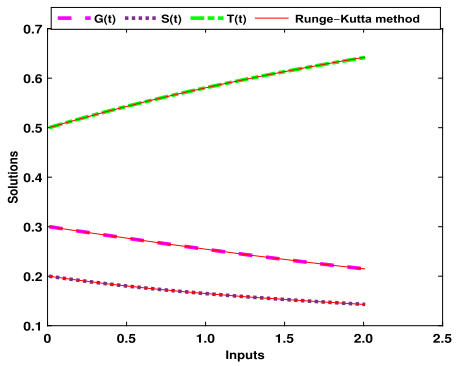

(a) Solution of Scenario 2

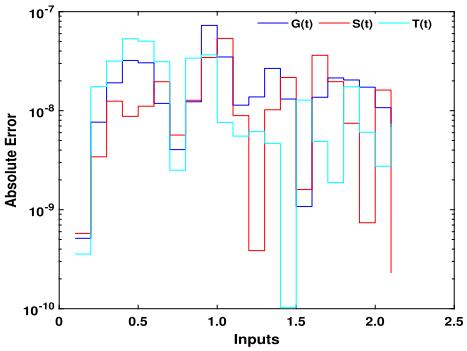

(b) Absolute errors of Scenario 2

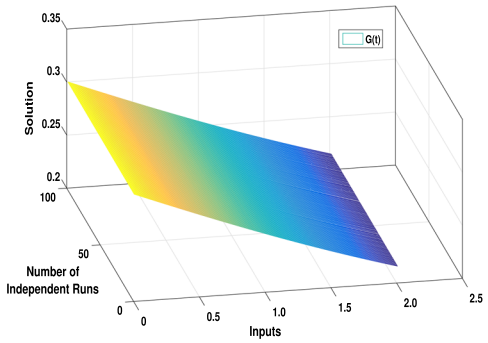

(c) Solutions of 100 independent Runs of $G(t)$

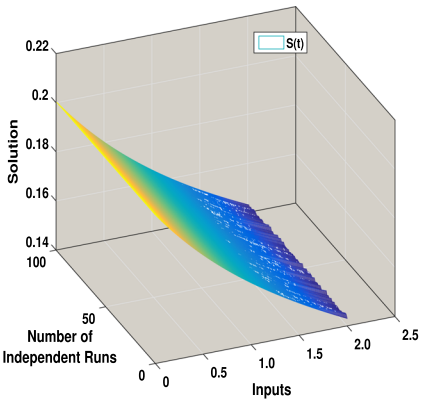

(d) Solutions of 100 independent Runs of $S(t)$

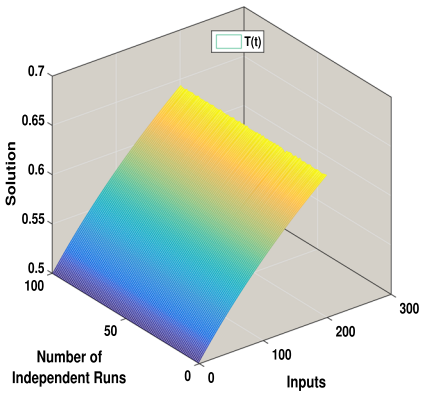

(e) Solutions of 100 independent Runs of $T(t)$

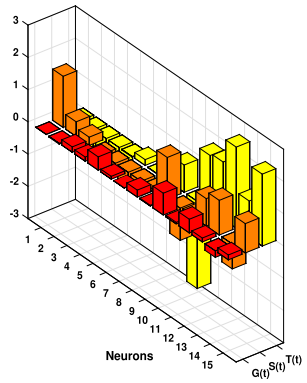

(f) Weights found by ANN-SCA-IPA

Fig. 4 Graphical representation of Scenario 2

the solution overlapped with the reference solution of Range-Kutta order 4 (RK4). This overlapping validates convergence of the proposed technique. The solution is written up to 9 decimal places to avoid round-off errors. The solution is obtained in $t \in [0, 2]$ with 0.01 step size having 201 input points.

4.2 Scenario 2

This scenario is based on the following values, of SES model in Eq. (2), birth rate of saplings $\beta = 0.5$, death rate of sapling $\mu = 0.01$, death rate of trees $v = 0.05$ and sapling to tree recruitment $\omega = 0.6$. Multiple executions are done for the SES model to collect a large number of data. The fitness function with 10 input points can be updated as:

$$E = \frac{1}{10}\sum_{i=1}^{10}\left(\left(\frac{dG_i}{dt} - 0.01S_i - 0.05T_i + 0.5G_iT_i\right)^2 + \left(\frac{dS_i}{dt} - 0.5G_iT_i + 0.6S_i + 0.01S_i\right)^2 + \left(\frac{dT_i}{dt} - 0.6S + 0.05T_i\right)^2\right) + \frac{1}{3}\left((G_i - 0.3)^2 + (S_i - 0.2)^2 + (T_i - 0.5)^2\right), \tag{26}$$

and the associated initial conditions are $G(0) = 0.3, S(0) = 0.2$ and $T(0) = 0.5$.

The sum of mean square errors of each equation is minimized by ANN-SCA-IPA technique. The solution obtained by ANN-SCA-IPA is compared graphically with the results of Range-Kutta order (RK4) in Fig. 4(a). The RK4 is implemented using Matlab's built-in function, Ode45. Each variable is plotted for 100 independent runs in sub-figure 4(c), (d) and (e). The solutions of RK4 are taken as a reference solution. The absolute errors between reference solution and solution by ANN-SCA-IPA algorithm are also drawn in Fig. 4(b). For evaluation of fitness values, statistical terms maximum (MAX), minimum (MIN), and standard deviation (STD) are used. The data for MAX, MIN, and STD is reported in Table 3. The values of minimum for all variables are in between 10^{-07} and 10^{-10}, the values of maximum are lies in 10^{-05} and 10^{-06}, the value of mean is in 10^{-05} and 10^{-06} and the values of standard deviation lies in 10^{-06} and 10^{-07}. The weights are drawn three-dimensionally given in sub-figure 3(f). The best weights found by execution of ANN-SCA-IPA technique are used in Eq. (6) which give the solution for SES model is given as:

$$\begin{aligned}
\hat{G}(t) &= \frac{-0.004378288}{1 + e^{-(1.587035916t - 0.148043677)}} + \frac{-0.025945658}{1 + e^{-(0.453549581t - 0.736097235)}} + \frac{0.16639304}{1 + e^{-(0.255518818t - 0.588822126)}} + \frac{0.130081459}{1 + e^{-(-0.481869439t - 0.586472007)}} + \frac{0.413067642}{1 + e^{-(-0.378362849t - 0.019243871)}},\\
\hat{S}(t) &= \frac{0.088065116}{1 + e^{-(-0.427043027t + 0.179209671)}} + \frac{0.010942248}{1 + e^{-(-0.448523782t - 0.013473171)}} + \frac{0.216601033}{1 + e^{-(-0.064374122t - 0.389150715)}} + \frac{0.024022748}{1 + e^{-(1.292927779t + 0.844812814)}} + \frac{0.676018771}{1 + e^{-(-0.999146969t - 2.70669461)}},\\
\hat{T}(t) &= \frac{0.050232974}{1 + e^{-(0.035892504t + 1.696553107)}} + \frac{0.424904706}{1 + e^{-(0.850659841t + 1.771509205)}} + \frac{0.120106756}{1 + e^{-(1.075056645t + 2.513236609)}} + \frac{-0.201832625}{1 + e^{-(-0.773599858t + 1.120160969)}} + \frac{0.150034871}{1 + e^{-(0.908638301t + 2.231291339)}}
\end{aligned} \tag{27}$$

Table 3 Absolute errors of scenario 2 with reference solution

t	G(t)				S(t)			T(t)			
	MIN	MAX	MEAN	STD	MIN	MAX	MEAN	STD	MIN	MAX	MEAN	STD
1.0	1.10×10^{-07}	2.40×10^{-05}	1.88×10^{-06}	2.29×10^{-06}	5.37×10^{-08}	7.68×10^{-06}	2.03×10^{-06}	1.86×10^{-06}	7.61×10^{-09}	1.05×10^{-05}	1.50×10^{-06}	1.62×10^{-06}
1.1	1.05×10^{-09}	2.61×10^{-05}	1.92×10^{-06}	2.50×10^{-06}	8.92×10^{-09}	7.64×10^{-06}	1.98×10^{-06}	1.86×10^{-06}	5.53×10^{-09}	1.07×10^{-05}	1.50×10^{-06}	1.64×10^{-06}
1.2	1.22×10^{-07}	2.81×10^{-05}	1.94×10^{-06}	2.70×10^{-06}	3.86×10^{-10}	7.48×10^{-06}	1.89×10^{-06}	1.83×10^{-06}	6.15×10^{-09}	1.07×10^{-05}	1.48×10^{-06}	1.64×10^{-06}
1.3	2.58×10^{-07}	3.01×10^{-05}	1.93×10^{-06}	2.90×10^{-06}	1.02×10^{-08}	7.20×10^{-06}	1.77×10^{-06}	1.77×10^{-06}	4.68×10^{-09}	1.06×10^{-05}	1.44×10^{-06}	1.62×10^{-06}
1.4	4.05×10^{-07}	3.19×10^{-05}	1.90×10^{-06}	3.09×10^{-06}	2.16×10^{-08}	6.83×10^{-06}	1.64×10^{-06}	1.69×10^{-06}	1.02×10^{-10}	1.03×10^{-05}	1.37×10^{-06}	1.57×10^{-06}
1.5	4.21×10^{-07}	3.37×10^{-05}	1.85×10^{-06}	3.27×10^{-06}	1.60×10^{-09}	6.36×10^{-06}	1.49×10^{-06}	1.57×10^{-06}	1.28×10^{-08}	9.99×10^{-06}	1.30×10^{-06}	1.50×10^{-06}
1.6	2.98×10^{-07}	3.54×10^{-05}	1.79×10^{-06}	3.45×10^{-06}	3.62×10^{-08}	5.82×10^{-06}	1.35×10^{-06}	1.42×10^{-06}	4.89×10^{-09}	9.53×10^{-06}	1.21×10^{-06}	1.41×10^{-06}
1.7	1.65×10^{-07}	3.70×10^{-05}	1.71×10^{-06}	3.62×10^{-06}	1.96×10^{-08}	5.21×10^{-06}	1.20×10^{-06}	1.24×10^{-06}	1.88×10^{-09}	8.98×10^{-06}	1.12×10^{-06}	1.31×10^{-06}
1.8	2.33×10^{-08}	3.86×10^{-05}	1.62×10^{-06}	3.79×10^{-06}	7.46×10^{-09}	4.54×10^{-06}	1.05×10^{-06}	1.05×10^{-06}	1.75×10^{-08}	8.33×10^{-06}	1.01×10^{-06}	1.19×10^{-06}
1.9	8.08×10^{-08}	4.01×10^{-05}	1.52×10^{-06}	3.95×10^{-06}	7.38×10^{-10}	3.82×10^{-06}	9.09×10^{-07}	8.52×10^{-07}	6.05×10^{-09}	7.61×10^{-06}	9.05×10^{-07}	1.06×10^{-06}
2.0	3.95×10^{-08}	4.15×10^{-05}	1.41×10^{-06}	4.10×10^{-06}	1.62×10^{-08}	3.07×10^{-06}	7.65×10^{-07}	6.64×10^{-07}	2.75×10^{-09}	6.82×10^{-06}	7.92×10^{-07}	9.18×10^{-07}

the solution overlapped with the reference solution of Range-Kutta order 4 (RK4). This overlapping validates convergence of the proposed technique. The solution is written up to 9 decimal places to avoid round-off errors. The solution is obtained in $t \in [0, 2]$ with 0.01 step size having 201 input points.

4.3 Scenario 3

This scenario is based on the following values, of SES model in Eq. (2), birth rate of saplings $\beta = 0.7$, death rate of sapling $\mu = 0.2$, death rate of trees $v = 0.1$ and sapling to tree recruitment $\omega = 0.7$. Multiple executions are done for the SES model to collect a large number of data. The fitness function with 10 input points can be updated as:

$$E = \frac{1}{10}\sum_{i=1}^{10}\left(\left(\frac{dG_i}{dt} - 0.2S_i - 0.1T_i + 0.7G_iT_i\right)^2 + \left(\frac{dS_i}{dt} - 0.7G_iT_i + 0.7S_i + 0.2S_i\right)^2 + \left(\frac{dT_i}{dt} - 0.7S + 0.1T_i\right)^2\right) + \frac{1}{3}\left((G_i - 0.5)^2 + (S_i - 0.3)^2 + (T_i - 0.2)^2\right), \tag{28}$$

and the associated initial conditions are $G(0) = 0.5, S(0) = 0.3$ and $T(0) = 0.2$.

The sum of mean square errors of each equation is minimized by ANN-SCA-IPA technique. The solution obtained by ANN-SCA-IPA is compared graphically with the results of Range-Kutta order (RK4) in Fig. 5(a). The RK4 is implemented using Matlab's built-in function, Ode45. Each variable is plotted for 100 independent runs in sub-figure 5(c), (d) and (e). The solutions of RK4 are taken as a reference solution. The absolute errors between reference solution and solution by ANN-SCA-IPA algorithm are also drawn in Fig. 5(b). For evaluation of fitness values, statistical terms maximum (MAX), minimum (MIN), and standard deviation (STD) are used. The data for MAX, MIN, and STD is reported in Table 4. The minimum values for all variables are in between 10^{-08} and 10^{-11}, the maximum values are about 10^{-06}, the value of mean is in 10^{-06} and 10^{-07} and the values of standard deviation lies in 10^{-06} and 10^{-07}. The weights are drawn three-dimensionally given in sub-figure 5(f). The best weights found by execution of ANN-SCA-IPA technique are used in Eq. (6) which give the solution for SES model is given as:

Fig. 5 Graphical representation of Scenario 3

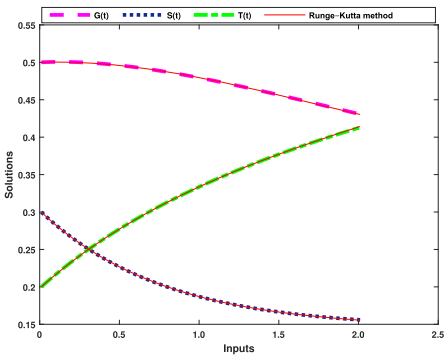

(a) Solution of Scenario 3

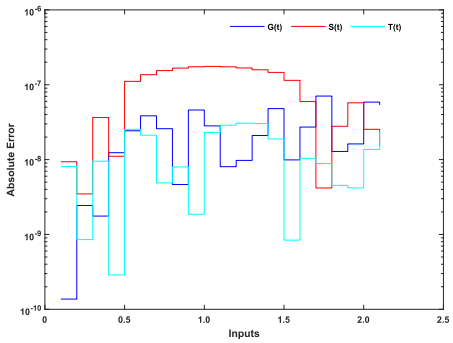

(b) Absolute errors of Scenario 3

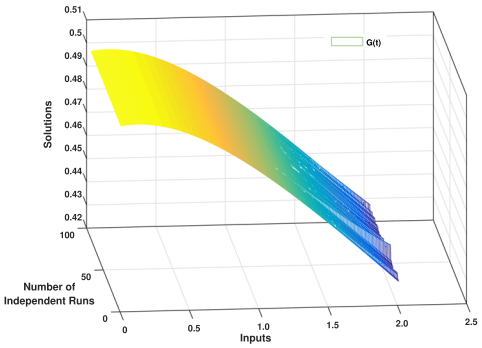

(c) Solutions of 100 independent Runs of $G(t)$

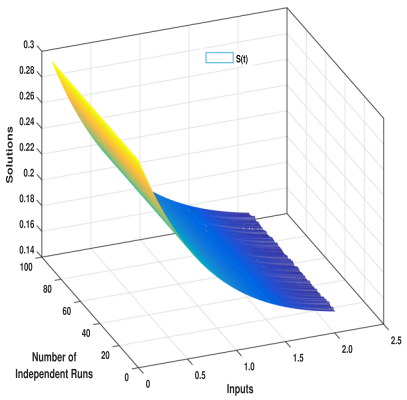

(d) Solutions of 100 independent Runs of $S(t)$

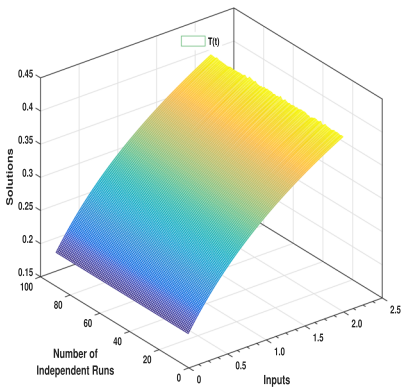

(e) Solutions of 100 independent Runs of $T(t)$

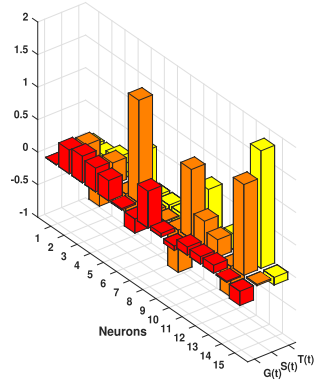

(f) Weights found by ANN-SCA-IPA

Table 4 Absolute errors of scenario 3 with reference solution

t	G(t)				S(t)			T(t)			
	MIN	MAX	MEAN	STD	MIN	MAX	MEAN	STD	MIN	MAX	MEAN	STD
1.0	2.72×10^{-09}	4.97×10^{-06}	1.05×10^{-06}	8.22×10^{-07}	3.47×10^{-09}	4.57×10^{-06}	8.64×10^{-07}	7.20×10^{-07}	5.47×10^{-08}	3.46×10^{-06}	1.27×10^{-06}	7.68×10^{-07}
1.1	3.58×10^{-09}	4.93×10^{-06}	9.43×10^{-07}	7.90×10^{-07}	2.45×10^{-08}	4.45×10^{-06}	7.00×10^{-07}	6.52×10^{-07}	9.26×10^{-10}	2.93×10^{-06}	1.02×10^{-06}	6.34×10^{-07}
1.2	4.13×10^{-09}	4.80×10^{-06}	8.18×10^{-07}	7.51×10^{-07}	5.23×10^{-09}	4.26×10^{-06}	5.28×10^{-07}	5.78×10^{-07}	6.14×10^{-09}	2.30×10^{-06}	7.40×10^{-07}	4.93×10^{-07}
1.3	7.58×10^{-10}	4.61×10^{-06}	6.87×10^{-07}	7.06×10^{-07}	1.16×10^{-09}	3.98×10^{-06}	3.69×10^{-07}	5.11×10^{-07}	2.93×10^{-09}	2.47×10^{-06}	4.55×10^{-07}	3.86×10^{-07}
1.4	1.41×10^{-08}	4.34×10^{-06}	5.74×10^{-07}	6.51×10^{-07}	6.71×10^{-10}	3.65×10^{-06}	2.90×10^{-07}	4.59×10^{-07}	1.30×10^{-08}	2.76×10^{-06}	2.82×10^{-07}	3.36×10^{-07}
1.5	1.33×10^{-09}	4.02×10^{-06}	4.89×10^{-07}	6.01×10^{-07}	3.15×10^{-09}	3.26×10^{-06}	3.68×10^{-07}	4.32×10^{-07}	1.53×10^{-08}	2.97×10^{-06}	4.41×10^{-07}	3.75×10^{-07}
1.6	4.29×10^{-11}	3.64×10^{-06}	4.93×10^{-07}	5.29×10^{-07}	5.25×10^{-09}	2.81×10^{-06}	5.46×10^{-07}	4.30×10^{-07}	1.99×10^{-08}	3.11×10^{-06}	7.49×10^{-07}	4.78×10^{-07}
1.7	1.29×10^{-08}	3.22×10^{-06}	5.34×10^{-07}	4.95×10^{-07}	1.60×10^{-08}	2.33×10^{-06}	7.40×10^{-07}	4.74×10^{-07}	9.54×10^{-09}	3.17×10^{-06}	1.07×10^{-06}	6.26×10^{-07}
1.8	4.57×10^{-09}	2.76×10^{-06}	5.91×10^{-07}	5.20×10^{-07}	1.78×10^{-08}	2.42×10^{-06}	9.30×10^{-07}	5.59×10^{-07}	2.68×10^{-08}	3.16×10^{-06}	1.39×10^{-06}	7.93×10^{-07}
1.9	8.27×10^{-09}	2.27×10^{-06}	6.72×10^{-07}	5.82×10^{-07}	1.27×10^{-08}	2.97×10^{-06}	1.11×10^{-06}	6.68×10^{-07}	1.85×10^{-08}	3.35×10^{-06}	1.69×10^{-06}	9.64×10^{-07}
2.0	7.60×10^{-09}	2.44×10^{-06}	7.64×10^{-07}	6.69×10^{-07}	3.22×10^{-08}	3.47×10^{-06}	1.28×10^{-06}	7.79×10^{-07}	2.02×10^{-08}	3.87×10^{-06}	1.97×10^{-06}	1.13×10^{-06}

$$
\begin{aligned}
\hat{G}(t) &= \frac{0.003954746}{1+\mathrm{e}^{-(-0.1248791t+0.073319745)}} \\
&+ \frac{0.36515532}{1+\mathrm{e}^{-(0.33679257t+0.074773987)}} \\
&+ \frac{0.409171459}{1+\mathrm{e}^{-(-0.465902062t+0.170550712)}} \\
&+ \frac{0.365152882}{1+\mathrm{e}^{-(0.33679916t+0.074776638)}} \\
&+ \frac{0.312424795}{1+\mathrm{e}^{-(-0.274818782t+0.536790222)}}, \\
\hat{S}(t) &= \frac{0.021485813}{1+\mathrm{e}^{-(1.578326589t-0.077437246)}} \\
&+ \frac{-0.21726037}{1+\mathrm{e}^{-(-0.263765816t-0.173708626)}} \\
&+ \frac{0.565280061}{1+\mathrm{e}^{-(-0.015711639t-0.50219569)}} \\
&+ \frac{0.055967561}{1+\mathrm{e}^{-(-0.65005606t-0.57764321)}} \\
&+ \frac{-0.067333053}{1+\mathrm{e}^{-(1.070519433t+0.657486063)}}, \\
\hat{T}(t) &= \frac{0.125124335}{1+\mathrm{e}^{-(0.41478089t-0.026378504)}} \\
&+ \frac{0.115908793}{1+\mathrm{e}^{-(0.269038758t+0.236769427)}} \\
&+ \frac{0.122375154}{1+\mathrm{e}^{-(-0.469744931t+0.056065942)}} \\
&+ \frac{0.015572656}{1+\mathrm{e}^{-(1.395145772t+1.806917576)}} \\
&+ \frac{-0.218318242}{1+\mathrm{e}^{-(-0.019361498t-0.116651107)}},
\end{aligned}
\tag{29}
$$

the solution overlapped with the reference solution of Range-Kutta order 4 (RK4). This overlapping validates convergence of the proposed technique. The solution is written up to 9 decimal places to avoid round-off errors. The solution is obtained in $t \in [0, 2]$ with 0.01 step size having 201 input points.

4.4 Scenario 4

This scenario is based on the following values, of SES model in Eq. (2), birth rate of saplings $\beta = 0.7$, death rate of sapling $\mu = 0.3$, death rate of trees $v = 0.2$ and sapling to tree recruitment $\omega = 0.5$. Multiple executions are done for SES model to collect a large number of data. The fitness function with 10 input points can be updated as:

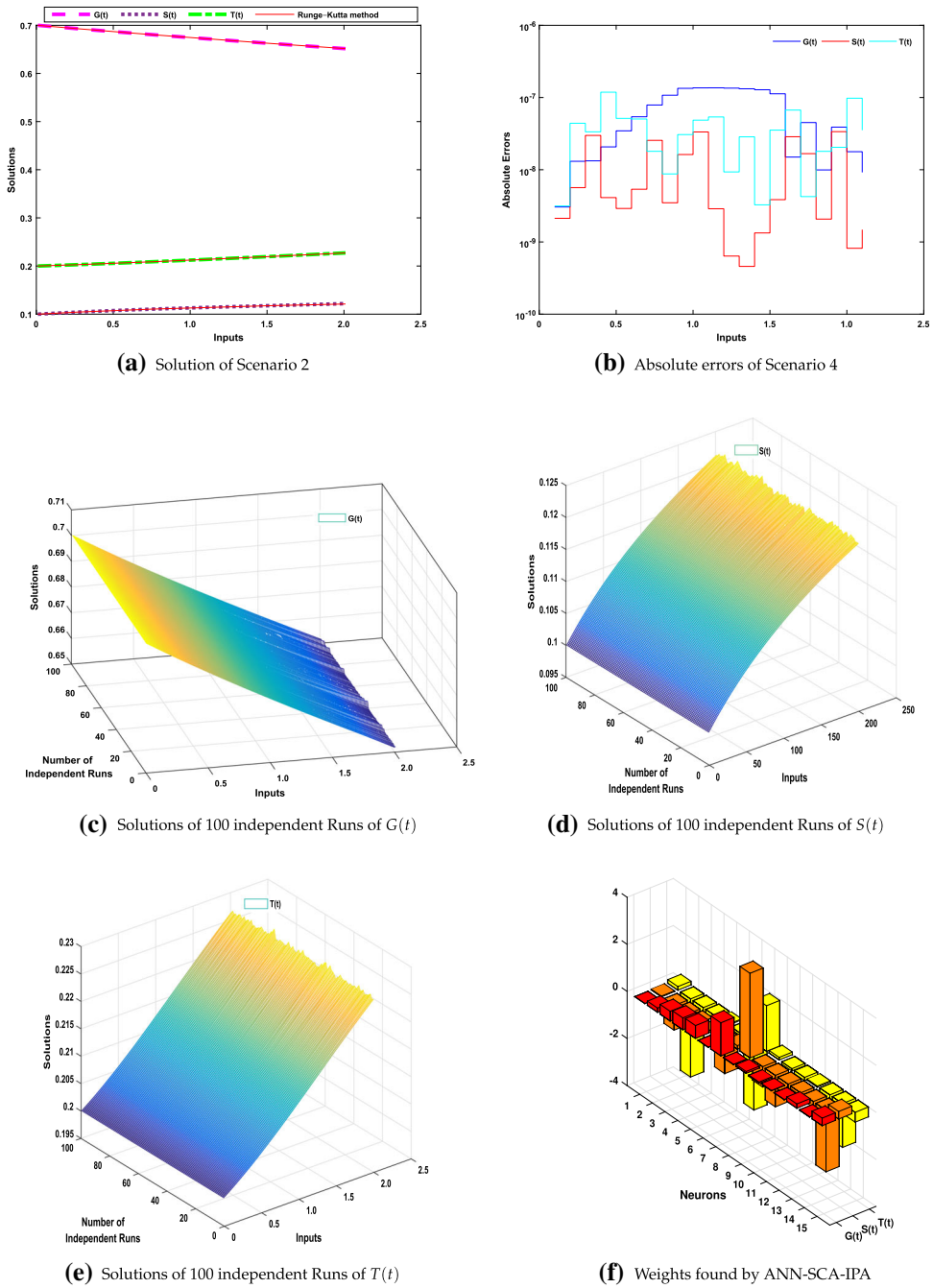

Fig. 6 Graphical representation of Scenario 4

(a) Solution of Scenario 2

(b) Absolute errors of Scenario 4

(c) Solutions of 100 independent Runs of $G(t)$

(d) Solutions of 100 independent Runs of $S(t)$

(e) Solutions of 100 independent Runs of $T(t)$

(f) Weights found by ANN-SCA-IPA

$$
\begin{aligned}
E = \frac{1}{10}\sum_{i=1}^{10}\Bigg(&\left(\frac{dG_i}{dt} - 0.3S_i - 0.2T_i + 0.7G_iT_i\right)^2 \\
&+\left(\frac{dS_i}{dt} - 0.7G_iT_i + 0.5S_i + 0.3S_i\right)^2 \\
&+\left(\frac{dT_i}{dt} - 0.5S_i + 0.2T_i\right)^2\Bigg) \\
&+\frac{1}{3}\left((G_i - 0.7)^2 + (S_i - 0.1)^2 + (T_i - 0.2)^2\right),
\end{aligned}
\tag{30}
$$

and the associated initial conditions are $G(0) = 0.7, S(0) = 0.1$ and $T(0) = 0.2$.

The sum of mean square errors of each equation is minimized by ANN-SCA-IPA technique. The solution obtained by ANN-SCA-IPA is compared graphically with the results of Range-Kutta order (RK4) in Fig. 6(a). The RK4 is implemented using Matlab's built-in function, Ode45. Each variable is plotted for 100 independent runs in sub-figure 6(c), (d) and (e). The solutions of RK4 are taken as a reference solution. The absolute errors between

Table 5 Absolute errors of scenario 4 with reference solution

t	G(t)				S(t)			T(t)			
	MIN	MAX	MEAN	STD	MIN	MAX	MEAN	STD	MIN	MAX	MEAN	STD
1.0	1.36×10^{-07}	1.98×10^{-05}	2.02×10^{-06}	3.48×10^{-06}	3.34×10^{-08}	4.92×10^{-06}	1.55×10^{-06}	1.36×10^{-06}	4.86×10^{-08}	4.81×10^{-06}	2.44×10^{-06}	9.76×10^{-07}
1.1	1.36×10^{-07}	2.11×10^{-05}	2.08×10^{-06}	3.72×10^{-06}	2.89×10^{-09}	5.02×10^{-06}	1.54×10^{-06}	1.37×10^{-06}	5.39×10^{-08}	4.93×10^{-06}	2.49×10^{-06}	1.00×10^{-06}
1.2	1.35×10^{-07}	2.23×10^{-05}	2.12×10^{-06}	3.93×10^{-06}	6.38×10^{-10}	5.04×10^{-06}	1.52×10^{-06}	1.35×10^{-06}	9.33×10^{-09}	4.97×10^{-06}	2.49×10^{-06}	1.02×10^{-06}
1.3	1.32×10^{-07}	2.33×10^{-05}	2.14×10^{-06}	4.12×10^{-06}	4.59×10^{-10}	4.98×10^{-06}	1.47×10^{-06}	1.31×10^{-06}	2.86×10^{-08}	4.95×10^{-06}	2.46×10^{-06}	1.02×10^{-06}
1.4	1.28×10^{-07}	2.42×10^{-05}	2.13×10^{-06}	4.29×10^{-06}	1.33×10^{-09}	4.86×10^{-06}	1.41×10^{-06}	1.24×10^{-06}	3.27×10^{-09}	4.86×10^{-06}	2.40×10^{-06}	1.02×10^{-06}
1.5	1.13×10^{-07}	2.49×10^{-05}	2.11×10^{-06}	4.43×10^{-06}	3.85×10^{-09}	4.67×10^{-06}	1.33×10^{-06}	1.16×10^{-06}	3.54×10^{-08}	4.73×10^{-06}	2.32×10^{-06}	9.94×10^{-07}
1.6	1.50×10^{-08}	2.55×10^{-05}	2.06×10^{-06}	4.55×10^{-06}	2.87×10^{-08}	4.43×10^{-06}	1.24×10^{-06}	1.06×10^{-06}	6.71×10^{-08}	4.54×10^{-06}	2.21×10^{-06}	9.58×10^{-07}
1.7	4.50×10^{-08}	2.60×10^{-05}	2.00×10^{-06}	4.64×10^{-06}	1.67×10^{-08}	4.14×10^{-06}	1.14×10^{-06}	9.70×10^{-07}	4.25×10^{-09}	4.31×10^{-06}	2.08×10^{-06}	9.15×10^{-07}
1.8	9.94×10^{-09}	2.63×10^{-05}	1.93×10^{-06}	4.71×10^{-06}	2.07×10^{-09}	3.80×10^{-06}	1.02×10^{-06}	8.73×10^{-07}	1.80×10^{-08}	4.04×10^{-06}	1.93×10^{-06}	8.59×10^{-07}
1.9	3.89×10^{-08}	2.65×10^{-05}	1.84×10^{-06}	4.76×10^{-06}	3.37×10^{-08}	3.43×10^{-06}	9.08×10^{-07}	7.82×10^{-07}	2.04×10^{-08}	3.73×10^{-06}	1.76×10^{-06}	7.94×10^{-07}
2.0	1.78×10^{-08}	2.66×10^{-05}	1.75×10^{-06}	4.79×10^{-06}	8.18×10^{-10}	3.02×10^{-06}	7.88×10^{-07}	7.08×10^{-07}	9.78×10^{-08}	3.39×10^{-06}	1.58×10^{-06}	7.24×10^{-07}

reference solution and solution by ANN-SCA-IPA algorithm are also drawn in Fig. 6(b). For evaluation of fitness values, statistical terms maximum (MAX), minimum (MIN), and standard deviation (STD) are used. The data for MAX, MIN, and STD is reported in Table 5. The values of minimum for all variables are in between 10^{-07} and 10^{-10}, the values of maximum are lies in 10^{-05} and 10^{-06}, the value of mean is in 10^{-06} and 10^{-07} and the values of standard deviation lies in 10^{-06} and 10^{-07}. The weights are drawn three-dimensionally given in sub-figure 6(f). The best weights found by execution of ANN-SCA-IPA technique are used in Eq. (6) which give the solution for SES model is given as:

$$
\begin{aligned}
\hat{G}(t) &= \frac{0.000285473}{1+\mathrm{e}^{-(0.034457792t+0.153273689)}} \\
&\quad + \frac{0.17900599}{1+\mathrm{e}^{-(-1.043395645t-3.320135645)}} \\
&\quad + \frac{0.411025561}{1+\mathrm{e}^{-(-0.105776769t-0.227553661)}} \\
&\quad + \frac{0.504197801}{1+\mathrm{e}^{-(0.003241391t-0.16593974)}} \\
&\quad + \frac{0.54952614}{1+\mathrm{e}^{-(-0.082816048t+0.039148546)}} \\
\hat{S}(t) &= \frac{-0.007613071}{1+\mathrm{e}^{-(-1.408632539t-0.102224703)}} \\
&\quad + \frac{1.407868544}{1+\mathrm{e}^{-(0.151329609t-2.868084376)}} \\
&\quad + \frac{0.011815423}{1+\mathrm{e}^{-(3.596396568t+1.932350304)}} \\
&\quad + \frac{0.078964849}{1+\mathrm{e}^{-(-0.865975065t+0.109845808)}} \\
&\quad + \frac{-0.050513424}{1+\mathrm{e}^{-(-1.336373484t-0.09673791)}} \\
\hat{T}(t) &= \frac{0.014326173}{1+\mathrm{e}^{-(-0.514447744t-0.139236015)}} \\
&\quad + \frac{-0.011003623}{1+\mathrm{e}^{-(-0.122231632t-0.046199967)}} \\
&\quad + \frac{0.182454552}{1+\mathrm{e}^{-(-0.252918437t-0.485000449)}} \\
&\quad + \frac{0.007639639}{1+\mathrm{e}^{-(-2.614707161t+-1.8629168)}} \\
&\quad + \frac{0.322741854}{1+\mathrm{e}^{-(0.319833727t-0.417641998)}}
\end{aligned}
\tag{31}
$$

The solution overlapped with the reference solution of Range-Kutta order 4 (RK4). This overlapping validates convergence of the proposed technique. The solution is written up to 9 decimal places to avoid round-off errors. The solution is obtained in $t \in [0, 2]$ with 0.01 step size having 201 input points.

4.5 Scenario 5

This scenario is based on the following values, of SES model in Eq. (2), birth rate of saplings $\beta = 0.7$, death rate of sapling $\mu = 0.2$, death rate of trees $\nu = 0.1$ and sapling to tree recruitment $\omega = 0.6$. Multiple executions are done for SES model to collect a large number of data. The fitness function with 10 input points can be updated as:

$$E = \frac{1}{10}\sum_{i=1}^{10}\left(\left(\frac{dG_i}{dt} - 0.2S_i - 0.1T_i + 0.7G_iT_i\right)^2 + \left(\frac{dS_i}{dt} - 0.7G_iT_i + 0.6S_i + 0.2S_i\right)^2 + \left(\frac{dT_i}{dt} - 0.6S + 0.1T_i\right)^2\right) + \frac{1}{3}\left((G_i - 0.6)^2 + (S_i - 0.1)^2 + (T_i - 0.2)^2\right), \tag{32}$$

and the associated initial conditions are $G(0) = 0.6, S(0) = 0.1$ and $T(0) = 0.3$.

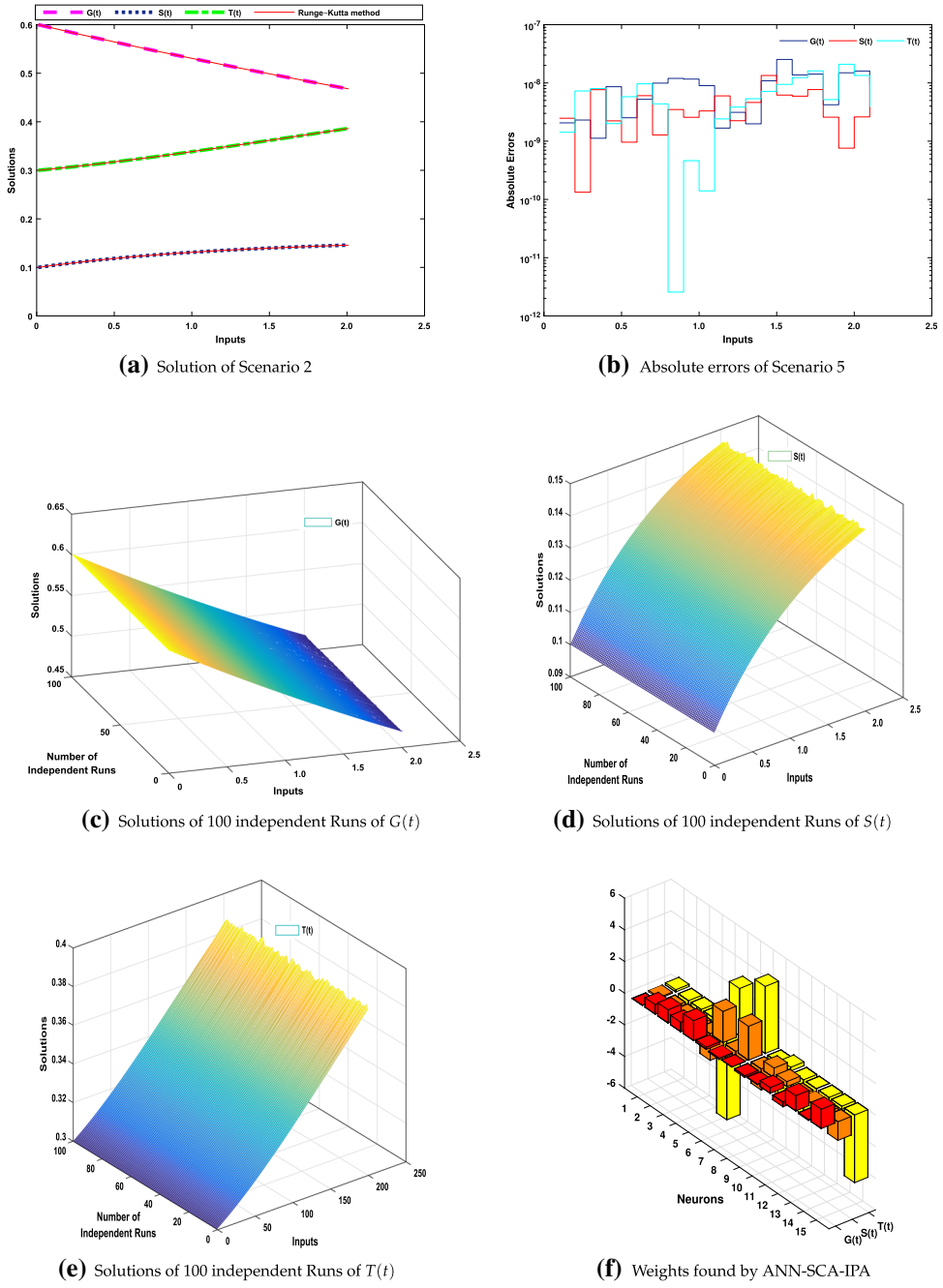

Fig. 7 Graphical representation of Scenario 5

(a) Solution of Scenario 2

(b) Absolute errors of Scenario 5

(c) Solutions of 100 independent Runs of $G(t)$

(d) Solutions of 100 independent Runs of $S(t)$

(e) Solutions of 100 independent Runs of $T(t)$

(f) Weights found by ANN-SCA-IPA

Table 6 Absolute errors of scenario 5 with reference solution

t	G(t)				S(t)				T(t)			
	MIN	MAX	MEAN	STD	MIN	MAX	MEAN	STD	MIN	MAX	MEAN	STD
1.0	8.98×10^{-09}	4.40×10^{-06}	1.17×10^{-06}	8.98×10^{-07}	3.30×10^{-09}	5.90×10^{-06}	9.89×10^{-07}	1.35×10^{-06}	1.40×10^{-10}	1.04×10^{-05}	3.00×10^{-06}	3.21×10^{-06}
1.1	1.68×10^{-09}	4.43×10^{-06}	1.17×10^{-06}	9.05×10^{-07}	6.00×10^{-09}	5.84×10^{-06}	9.61×10^{-07}	1.33×10^{-06}	2.41×10^{-09}	1.06×10^{-05}	3.01×10^{-06}	3.27×10^{-06}
1.2	3.13×10^{-09}	4.40×10^{-06}	1.16×10^{-06}	8.99×10^{-07}	2.25×10^{-09}	5.67×10^{-06}	9.29×10^{-07}	1.30×10^{-06}	3.85×10^{-09}	1.06×10^{-05}	2.98×10^{-06}	3.28×10^{-06}
1.3	1.99×10^{-09}	4.30×10^{-06}	1.13×10^{-06}	8.81×10^{-07}	4.62×10^{-09}	5.41×10^{-06}	8.98×10^{-07}	1.23×10^{-06}	5.36×10^{-09}	1.04×10^{-05}	2.91×10^{-06}	3.25×10^{-06}
1.4	1.09×10^{-08}	4.15×10^{-06}	1.09×10^{-06}	8.53×10^{-07}	1.34×10^{-08}	5.07×10^{-06}	8.72×10^{-07}	1.15×10^{-06}	7.16×10^{-09}	1.02×10^{-05}	2.82×10^{-06}	3.16×10^{-06}
1.5	2.53×10^{-08}	3.95×10^{-06}	1.04×10^{-06}	8.14×10^{-07}	6.19×10^{-09}	4.65×10^{-06}	8.48×10^{-07}	1.06×10^{-06}	9.43×10^{-09}	9.78×10^{-06}	2.69×10^{-06}	3.04×10^{-06}
1.6	1.37×10^{-08}	3.70×10^{-06}	9.73×10^{-07}	7.68×10^{-07}	5.93×10^{-09}	4.18×10^{-06}	8.22×10^{-07}	9.55×10^{-07}	1.24×10^{-08}	9.29×10^{-06}	2.54×10^{-06}	2.88×10^{-06}
1.7	1.42×10^{-08}	3.41×10^{-06}	8.97×10^{-07}	7.17×10^{-07}	7.69×10^{-09}	3.70×10^{-06}	7.97×10^{-07}	8.57×10^{-07}	1.61×10^{-08}	8.70×10^{-06}	2.37×10^{-06}	2.69×10^{-06}
1.8	4.22×10^{-09}	3.09×10^{-06}	8.12×10^{-07}	6.62×10^{-07}	2.58×10^{-09}	3.17×10^{-06}	7.69×10^{-07}	7.72×10^{-07}	5.18×10^{-09}	8.02×10^{-06}	2.18×10^{-06}	2.47×10^{-06}
1.9	1.49×10^{-08}	2.73×10^{-06}	7.27×10^{-07}	5.96×10^{-07}	7.59×10^{-10}	3.06×10^{-06}	7.53×10^{-07}	6.97×10^{-07}	2.09×10^{-08}	7.27×10^{-06}	1.99×10^{-06}	2.22×10^{-06}
2.0	1.60×10^{-08}	2.36×10^{-06}	6.44×10^{-07}	5.22×10^{-07}	2.61×10^{-09}	3.51×10^{-06}	7.41×10^{-07}	6.50×10^{-07}	1.34×10^{-08}	6.45×10^{-06}	1.78×10^{-06}	1.95×10^{-06}

The sum of mean square errors of each equation is minimized by ANN-SCA-IPA technique. The solution obtained by ANN-SCA-IPA is compared graphically with the results of Range-Kutta order (RK4) in Fig. 7(a). The RK4 is implemented using Matlab's built-in function, Ode45. Each variable is plotted for 100 independent runs in sub-figure 7(c), (d) and (e). The solutions of RK4 are taken as a reference solution. The absolute errors between reference solution and solution by ANN-SCA-IPA algorithm are also drawn in Fig. 7(b). For evaluation of fitness values, statistical terms maximum (MAX), minimum (MIN), and standard deviation (STD) is used. The data for MAX, MIN, and STD is reported in Table 6. The values of minimum for all variables are in between 10^{-08} and 10^{-10}, the values of maximum are lies in 10^{-05} and 10^{-06}, the value of mean is in 10^{-06} and 10^{-07} and the values of standard deviation lies in 10^{-06} and 10^{-07}. The weights are drawn three-dimensionally given in sub-figure 7(f). The best weights found by execution of ANN-SCA-IPA technique are used in Eq. (6) which give the solution for SES model is given as:

$$
\begin{aligned}
\hat{G}(t) &= \frac{-.00000864}{1+\mathrm{e}^{-(0.070397567t+0.137777316)}} \\
&\quad + \frac{0.597836205}{1+\mathrm{e}^{-(-0.169566172t-0.283645036)}} \\
&\quad + \frac{0.83390279}{1+\mathrm{e}^{-(-0.274564794t-2.21855874)}} \\
&\quad + \frac{0.600041299}{1+\mathrm{e}^{-(-0.169646602t-0.283080401)}} \\
&\quad + \frac{1.255868545}{1+\mathrm{e}^{-(-1.67942891t-5.863505512)}}, \\
\hat{S}(t) &= \frac{0.136250965}{1+\mathrm{e}^{-(1.966070558t+2.99109318)}} \\
&\quad + \frac{-0.076308791}{1+\mathrm{e}^{-(-0.836378399t-0.412892046)}} \\
&\quad + \frac{0.00019821}{1+\mathrm{e}^{-(2.141200205t+4.23394353)}} \\
&\quad + \frac{-0.108645235}{1+\mathrm{e}^{-(-1.333649228t-2.024147204)}} \\
&\quad + \frac{0.02349783}{1+\mathrm{e}^{-(0.612854695t+0.237232271)}}, \\
\hat{T}(t) &= \frac{0.362794409}{1+\mathrm{e}^{-(0.313187451t-2.220495271)}} \\
&\quad + \frac{-0.292508604}{1+\mathrm{e}^{-(-0.378536771t-0.009799846)}} \\
&\quad + \frac{0.96358051}{1+\mathrm{e}^{-(0.03517345t-0.281962738)}} \\
&\quad + \frac{-0.04661323}{1+\mathrm{e}^{-(-0.291258935t-0.197342371)}} \\
&\quad + \frac{1.215766272}{1+\mathrm{e}^{-(-1.176238747t-4.273156164)}},
\end{aligned}
\tag{33}
$$

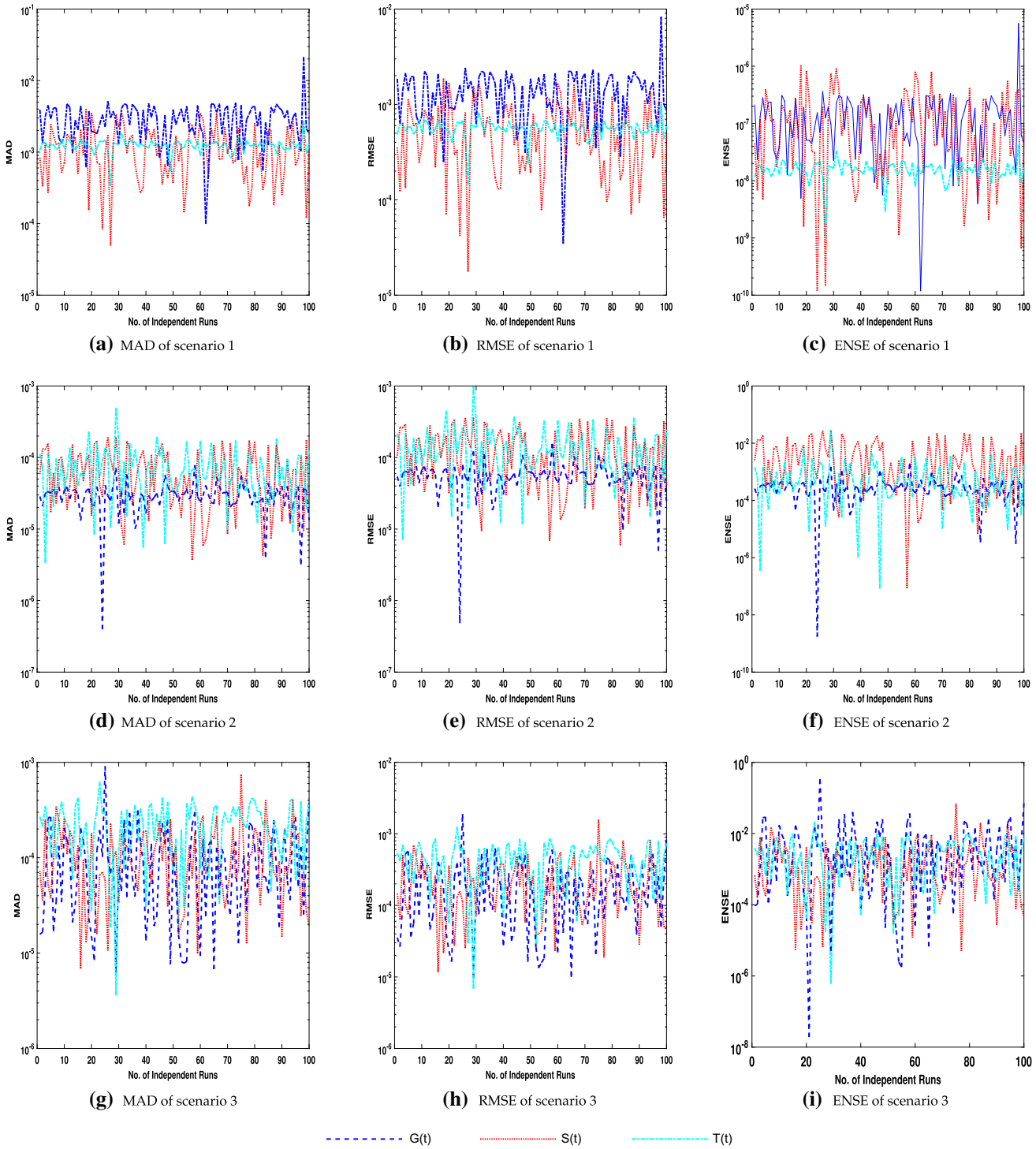

(a) MAD of scenario 1 **(b)** RMSE of scenario 1 **(c)** ENSE of scenario 1

(d) MAD of scenario 2 **(e)** RMSE of scenario 2 **(f)** ENSE of scenario 2

(g) MAD of scenario 3 **(h)** RMSE of scenario 3 **(i)** ENSE of scenario 3

Fig. 8 Graphs of performance operators

The solution overlapped with the reference solution of Range-Kutta order 4 (RK4). This overlapping validates convergence of the proposed technique. The solution is written up to 9 decimal places to avoid any round-off errors. The solution is obtained in $t \in [0, 2]$ with 0.01 step size having 201 input points.

4.6 Evaluation of ANN-SCA-IPA by performance matrices

For the performance evaluation of ANN-SCA-IPA technique, performance matrices are utilized. The utilized matrices are MAD, RMSE and ENSE. The definition of

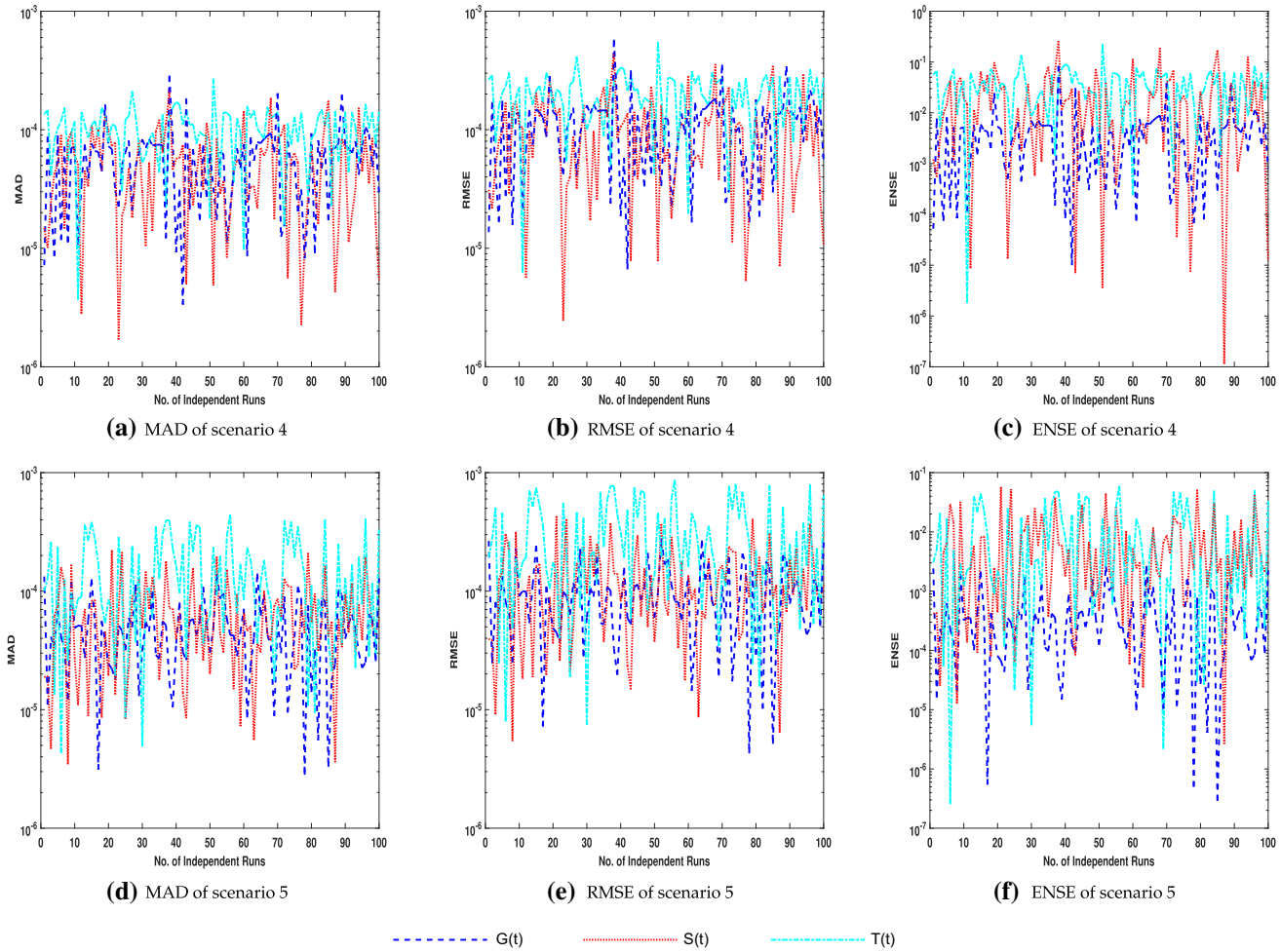

(a) MAD of scenario 4 **(b)** RMSE of scenario 4 **(c)** ENSE of scenario 4

(d) MAD of scenario 5 **(e)** RMSE of scenario 5 **(f)** ENSE of scenario 5

Fig. 9 Graphs of performance operators

these operators is given in Eqs. (21)-(23). The few runs(executions) cannot verify its consistency, reliability, and convergence. Therefore, ANN-SCA-IPA is executed 100 times to collect a large evaluation data set. The execution procedure SCA is executed to obtain its best weights and then provided to IPA as initial gauss for the refinement of provided variables. The values found for MAD, RMSE, and ENSE are drawn with the help of a line graph in Figs. 8, 9. In plotting the line graph, the y-axis is taken as a semi-log to observe the small variation in data. The operators MAD, RMSE and ENSE for scenario 1 are shown in Fig. 8(a), (b) and (c), for scenario 2 the values are shown in Fig. 8(d), (e) and (f), for scenario 3 are shown in Fig. 8(g), (h) and (i). With a similar pattern, scenario 4 and scenario 5 are given in Fig. 9. From Figs. 8 and 9, its observed that the values of MAD for scenario 1, scenario 2, scenario 3, scenario 4 and scenario 5 are between 10^{-03} to 10^{-07}, the values of RMSE are in between 10^{-03} to 10^{-06} and values of ENSE lies in 10^{-03} to 10^{-10}. Each sub-figure consist of three graphs each for variable $G(t)$, $S(t)$ and $T(t)$.

The best value of MAD, RMSE, and ENSE is zero. From Figs. 8 and 9, it seems that the values of MAD, RMSE, and ENSE converge to zero. The MAD, RMSE, and ENSE have impressive values. Which shows that the ANN-SCA-IPA technique is consistent and reliable for the solution of the SES model. Furthermore, the fitness value of each variable is also evaluated with Histogram having normal distribution and boxplots. The plots are given in Fig. 10. In Fig. 10, the sub-figure 10(a)-(c) shows the histogram for G(t), S(t) and T(t) of scenario 1, respectively. In similar pattern, the sub-figure 10(d)-(f) shows histogram for scenario 2. In sub-figure 10(e), (f) and (i) there are three boxplots each for G(t), S(t) and T(t) of scenario 3, 4 and 5, respectively. The boxplot shows five numerical values for each variable, i.e, minimum, first quartile, median, third quartile, and maximum. Which illustrate the fitness of solutions. The fitness values of all scenarios are statistically sound. The graphs show the consistency and reliability of ANN-SCA-IPA technique.

Moreover, for better visualization fitness of the proposed technique is drawn as a bar graph. The bar graphs are given

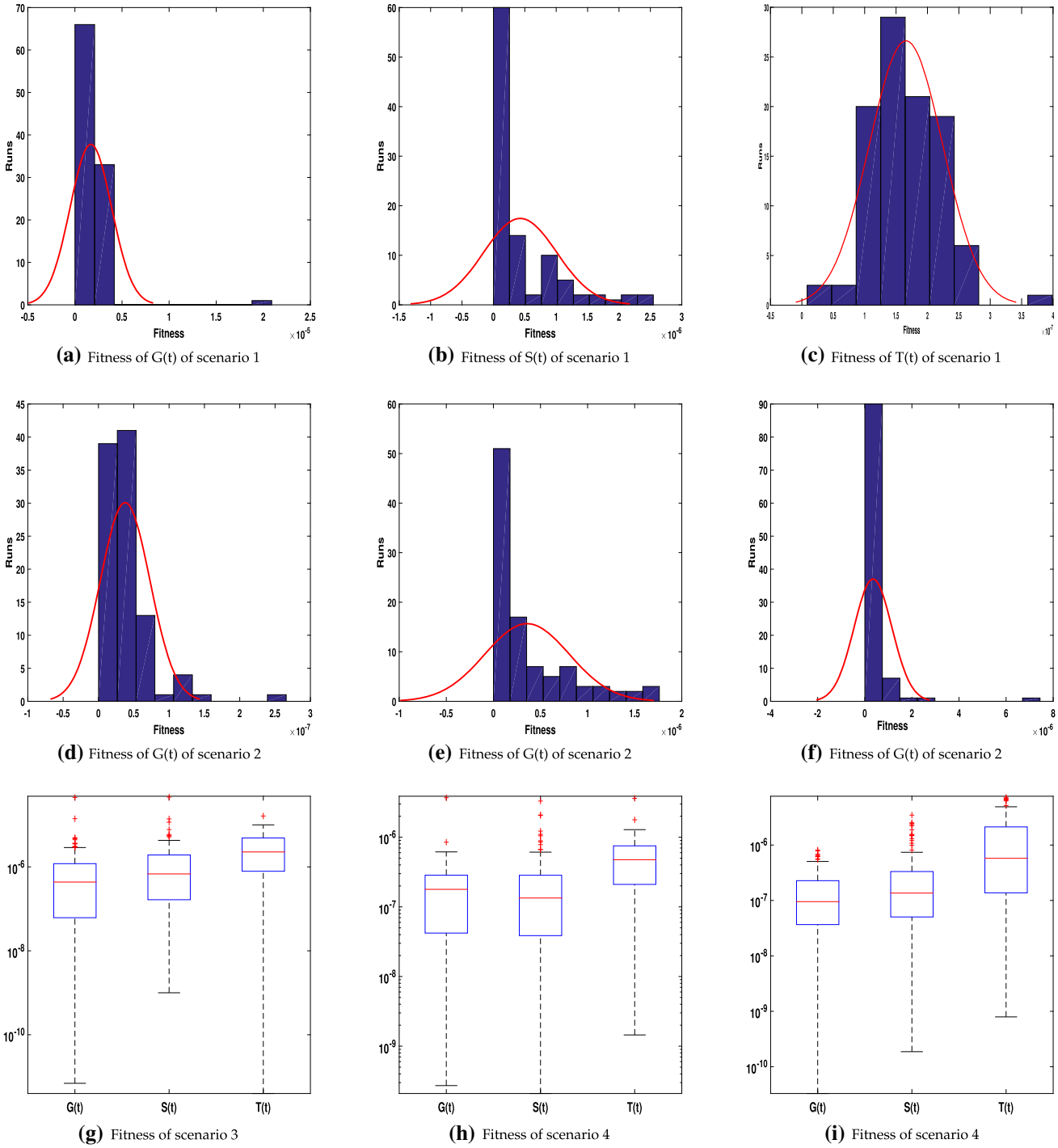

(a) Fitness of G(t) of scenario 1 **(b)** Fitness of S(t) of scenario 1 **(c)** Fitness of T(t) of scenario 1

(d) Fitness of G(t) of scenario 2 **(e)** Fitness of G(t) of scenario 2 **(f)** Fitness of G(t) of scenario 2

(g) Fitness of scenario 3 **(h)** Fitness of scenario 4 **(i)** Fitness of scenario 4

Fig. 10 Fitness evaluation by Histogram with normal distribution and Boxplots

in Fig. 11. Each bar graph shows the values best, worst, and mean for variables G(t), S(t), and T(t). The bar graphs are drawn with a log on y-axis. In each graph, it can seem that fitness value is considerably better. Even the worst value is less than 10^{-7}. These graphs give simple and more visual detail of fitness.

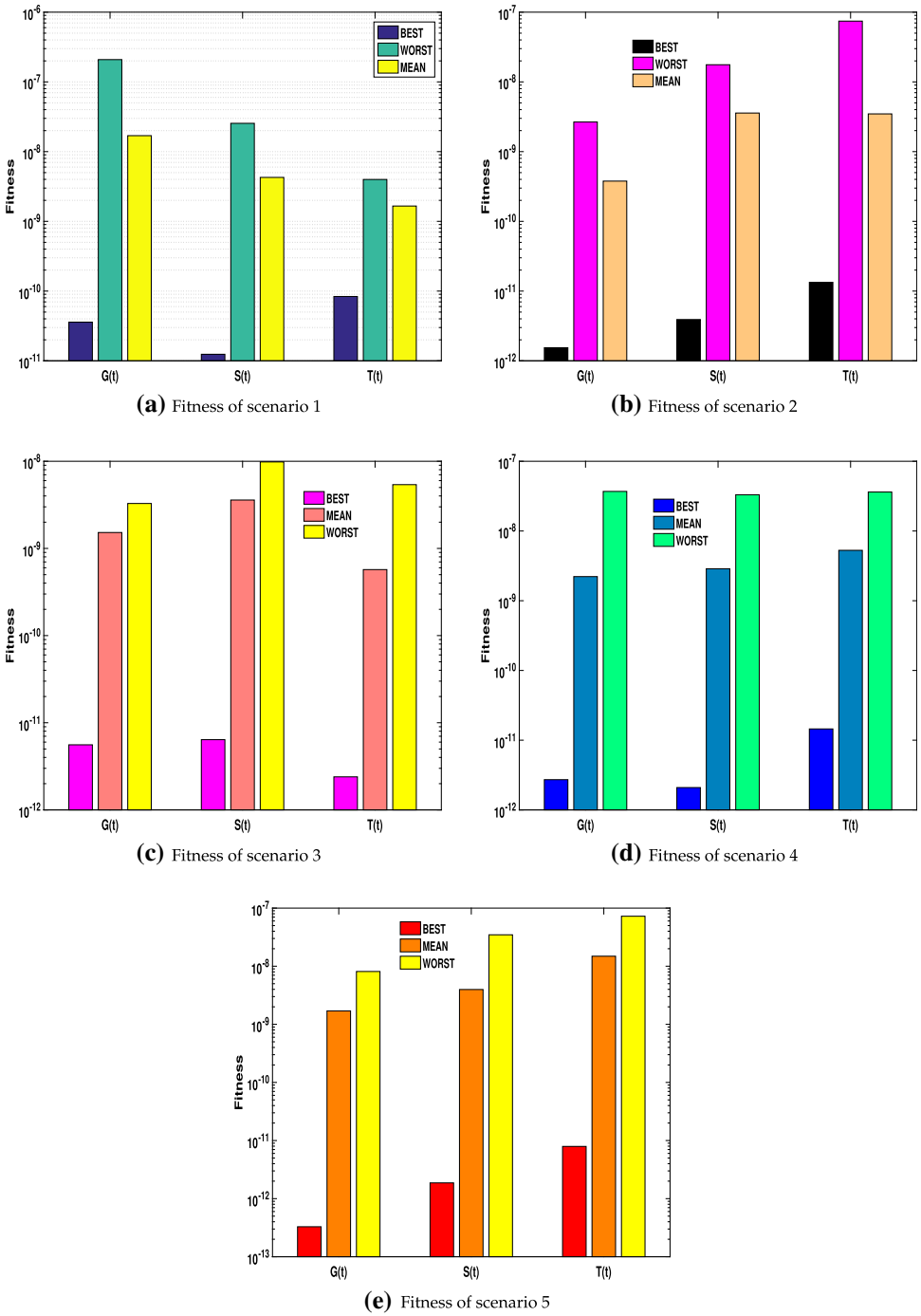

(a) Fitness of scenario 1

(b) Fitness of scenario 2

(c) Fitness of scenario 3

(d) Fitness of scenario 4

(e) Fitness of scenario 5

Fig. 11 Best, worst and mean value of fitness

4.7 Evaluation by global performance operators

The performance of ANN-SCA-IPA technique is evaluated by global variants of performance operators MAD, ENSE, and RMSE. Their global version is abbreviated as GMAD, GRMSE, and GENSE. The values of these global operators depend on the average values of MAD, RMSE, and ENSE. The definition of GMAD, GRMSE and GENSE are given in Eqs. (21–23), respectively. For each operator, the minimum(MIN) and mean values are reported in Table 7. In the table, the value of scenarios 1, 2, 3, 4, and 5 for each variable G(t), S(t), and T(t) is given. For Scenario 1 the

Table 7 Statistical data of global performance operators

Scenario	Operator	GMAD		GRMSE		GENSE	
	Variable	MIN	MEAN	MIN	MEAN	MIN	MEAN
1	**G(t)**	9.88×10^{-07}	3.10×10^{-05}	3.47×10^{-07}	1.45×10^{-05}	1.20×10^{-12}	1.95×10^{-09}
	S(t)	4.93×10^{-07}	1.31×10^{-05}	1.76×10^{-07}	6.04×10^{-06}	1.19×10^{-12}	1.70×10^{-09}
	T(t)	3.35×10^{-06}	1.25×10^{-05}	1.44×10^{-06}	5.68×10^{-06}	1.11×10^{-11}	1.62×10^{-10}
2	**G(t)**	3.99×10^{-09}	3.04×10^{-07}	4.83×10^{-09}	5.77×10^{-07}	1.74×10^{-11}	3.40×10^{-06}
	S(t)	3.70×10^{-08}	7.17×10^{-07}	5.94×10^{-08}	1.38×10^{-06}	8.63×10^{-10}	6.02×10^{-05}
	T(t)	3.34×10^{-08}	7.66×10^{-07}	7.08×10^{-08}	1.51×10^{-06}	8.33×10^{-10}	1.17×10^{-05}
3	**G(t)**	2.90×10^{-08}	5.35×10^{-07}	4.06×10^{-08}	1.06×10^{-06}	2.43×10^{-07}	2.32×10^{-04}
	S(t)	3.94×10^{-08}	7.81×10^{-07}	6.13×10^{-08}	1.52×10^{-06}	2.95×10^{-06}	2.01×10^{-04}
	T(t)	1.50×10^{-08}	2.91×10^{-07}	2.58×10^{-08}	5.50×10^{-07}	1.77×10^{-07}	1.41×10^{-04}
4	**G(t)**	3.34×10^{-08}	6.07×10^{-07}	6.64×10^{-08}	1.16×10^{-06}	1.00×10^{-07}	5.57×10^{-05}
	S(t)	1.70×10^{-08}	5.64×10^{-07}	2.45×10^{-08}	1.08×10^{-06}	1.14×10^{-09}	2.73×10^{-04}
	T(t)	3.67×10^{-08}	1.04×10^{-06}	6.21×10^{-08}	2.03×10^{-06}	1.80×10^{-08}	3.93×10^{-04}
5	**G(t)**	2.83×10^{-08}	5.09×10^{-07}	4.28×10^{-08}	9.94×10^{-07}	2.89×10^{-09}	4.96×10^{-06}
	S(t)	3.46×10^{-08}	6.82×10^{-07}	5.44×10^{-08}	1.33×10^{-06}	2.65×10^{-08}	8.60×10^{-05}
	T(t)	4.32×10^{-08}	1.55×10^{-06}	7.44×10^{-08}	3.05×10^{-06}	2.53×10^{-09}	1.18×10^{-04}

value of GMAD is between 10^{-06}–10^{-07}, GRMSE lies in 10^{-05}–10^{-07} and GENSE are in between 10^{-09}–10^{-12}. The values of GMAD for scenario 2 10^{-07}–10^{-09}, GRMSE has values 10^{-07}–10^{-09} and GENSE are 10^{-06}–10^{-11}. Similar values can observe for scenarios 3, 4, and 5 from Table 7. The values of all the operators are consistent, which verifies the consistency, reliability, and convergence of ANN-SCA-IPA technique.

4.8 Complexity analysis on the basis of 100 runs

The complexity of ANN-SCA-IPA technique is checked by plotting graphs of the solutions obtained for 100 runs. The graphs are given in Figs. 3–7. For all solutions, Mesh graph is plotted to study them collectively. A single run or few runs cannot justify the reliability of a technique. That's why multiple executions are done to collect a large data set.

Scenario 1

In the Fig. 3(c), (d) and (e) shows the solution for G(t), S(t) and T(t). From the figures, it can be observed that the graphs are smooth, and no jumps are there for all the variables. But in sub-figure 3(d), the solutions of variable S(t) are slightly disturbed as small jumps in the solutions are observed in the last digits.

Scenario 2

From Fig. 4(c), (d) and (e), the solutions of G(t), S(t) and T(t) can observe. No distraction is found in variables G(t) and T(t) solutions. A slight distraction can be observed in the solution of S(t) in very few values.

Scenario 3

In the Fig. 5(c), (d) and (e) shows the solution for G(t), S(t) and T(t). In Fig. 5(d), the solutions of S(t) are dismay. The solutions are distracted for last values. But for G(t) and T(t) are smooth, and no jumps are there.

Scenario42

Fig. 6(c), (d) and (e) shows the solutions variables. It can observe that the solutions are impressively consistent for all the runs. No interference is found in the solutions of G(t), S(t), and T(t) of scenario 4.

Scenario 5

Fig. 7(c), (d) and (e) shows the solutions variables. Similar to scenario 4, the solutions of G(t), S(t), and T(t) are consistent.

From the above discussion, it can conclude that performance of the ANN-SCA-IPA technique is impressive. Furthermore, the convergence rate of the proposed technique is high.

5 Conclusions

Savanna vegetation is an important component of the ecosystem. The increase and decrease in Savanna vegetation can cause disturbance to the ecosystem. The mathematical model of the Savanna ecosystem is considered. The model dynamics are evaluated by its parameters, such as the death rate of a sapling, the death rate of trees, and sapling to tree recruitment. The Savanna ecosystem model is given in the system (2). To solve the SES model (2), a hybridized technique of SCA and IPA is proposed with the

influence of ANN. For the solution of the SES model, mean square error based fitness function is designed given in Eqs. (9)-(13). For evaluation ANN-SCA-IPA technique, a large data set is collected by multiple runs. The fitness of the SES model is evaluated by convergence plots such as boxplots, bar graphs, and histograms with normal distribution. From all these evaluations, it can observe that ANN-SCA-IPA is robust and reliable. It can be implemented for many other physical, chemical, and biological models. In the future, the SES model's limitation can be modified with other assumptions like Savanna-fire, soil effect on Savanna, grass and sapling, and climate change for the protection of Savanna.

References

Accatino F, De Michele C, Vezzoli R, Donzelli D, Scholes RJ (2010) Tree-grass co-existence in savanna: interactions of rain and fire. J Theor Biol 267:235–242

Ahmad A, Sulaiman M, Alhindi A, Aljohani AJ (2020) Analysis of temperature profiles in longitudinal fin designs by a novel neuroevolutionary approach. IEEE Access 8:113285–113308

Atwell BJ, Kriedemann PE, Turnbull CG (1999) Plants in action: adaptation in nature, performance in cultivation. Macmillan Education AU, Australia

Banerjee S, Das D, John R (2022) Grassland-Woodland Transitions Over Decadal Timescales in the Terai-Duar Savanna and Grasslands of the Indian Subcontinent. *Available at SSRN 4054431*

Byrd RH, Hribar ME, Nocedal J (1999) An interior point algorithm for large-scale nonlinear programming. SIAM J Optim 9:877–900

Coetsee C, Wigley B, Sankaran M, Ratnam J, Augustine D (2022) Contrasting Effects of Grazing vs Browsing Herbivores Determine Changes in Soil Fertility in an East African Savanna. Ecosystems. https://doi.org/10.1007/s10021-022-00748-7

Drüke M (2022) Modeling biophysical feedbacks in the Earth system to investigate a fire-controlled hysteresis of tropical forests

Du HZF (2022) Suggestion to establish a nature reserve for protecting native savanna vegetation in hot dry valley of Jinshajiang. Yunnan. Biodiversity Science. p. 0

Evans RD, Ehleringer JR (1994) Water and nitrogen dynamics in an arid woodland. Oecologia 99:233–242

Fawad Khan M, Bonyah E, Alshammari FS, Ghufran SM, Sulaiman M (2022) Modelling and Analysis of Virotherapy of Cancer Using an Efficient Hybrid Soft Computing Procedure. Complexity. https://doi.org/10.1155/2022/9660746

February EC, Higgins SI (2010) The distribution of tree and grass roots in savannas in relation to soil nitrogen and water. South African J Bot 76:517–523

Frost P (1986) Responses of savannas to stress and disturbance: a proposal for a collaborative programme of research

Gardner TA (2006) Tree-grass coexistence in the Brazilian cerrado: demographic consequences of environmental instability. J Biogeogr 33:448–463

Guerrero-Sánchez Y, Umar M, Sabir Z, Guirao JL, Raja MAZ (2021) Solving a class of biological HIV infection model of latently infected cells using heuristic approach. Discrete Contin Dyn Syst-S 14:3611

Hamilton T, Archibald S, Woodborne S (2022) Historic changes in the fire-rainfall relationship at a woodland-savanna transition zone in southern Africa. African J Range Forage Sci 39:70–81

Hempson GP, February EC, Verboom GA (2007) Determinants of savanna vegetation structure: Insights from Colophospermum mopane. Aust Ecol 32:429–435

Higgins SI, Bond WJ, Trollope WS (2000) Fire, resprouting and variability: a recipe for grass-tree coexistence in savanna. J Ecol 88:213–229

Jeltsch F, Weber GE, Grimm V (2000) Ecological buffering mechanisms in savannas: a unifying theory of long-term tree-grass coexistence. Plant Ecol 150:161–171

Khan A, Sulaiman M, Alhakami H, Alhindi A (2020) Analysis of oscillatory behavior of heart by using a novel neuroevolutionary approach. IEEE Access 8:86674–86695

Khan NA, Sulaiman M, Tavera Romero CA, Alarfaj FK (2021) Theoretical Analysis on Absorption of Carbon Dioxide (CO2) into Solutions of Phenyl Glycidyl Ether (PGE) Using Nonlinear Autoregressive Exogenous Neural Networks. Molecules 26:6041

Khan MF, Sulaiman M, Romero CAT, Alkhathlan A (2021) Falkner-Skan Flow with Stream-Wise Pressure Gradient and Transfer of Mass over a Dynamic Wall. Entropy 23:1448

Khan MF, Sulaiman M, Tavera Romero CA, Alkhathlan A (2021) A Hybrid Metaheuristic Based on Neurocomputing for Analysis of Unipolar Electrohydrodynamic Pump Flow. Entropy 23:1513

Khan A, Stoy P, Joiner J, Baldocchi D, Verfaillie J, Chen M, Otkin J (2022) The diurnal dynamics of Gross Primary Productivity using observations from the Advanced Baseline Imager on the Geostationary Operational Environmental Satellite R Series at an oak savanna ecosystem. J Geophys Res Biogeosciences 127(3):e2021JG006701

Laio F, D'Odorico P, Ridolfi L (2006) An analytical model to relate the vertical root distribution to climate and soil properties. Geophys Res Lett. https://doi.org/10.1029/2006GL027331

Losey JE, Vaughan M (2006) The economic value of ecological services provided by insects. Bioscience 56:311–323

McLaren JR, Wilson SD, Peltzer DA (2004) Plant feedbacks increase the temporal heterogeneity of soil moisture. Oikos 107:199–205

Mirjalili S (2016) SCA: a sine cosine algorithm for solving optimization problems. Knowledge-Based Syst 96:120–133

Nieman WA, van Wilgen BW, Radloff FG, Tambling CJ, Leslie AJ (2021) Comparative use of adjoining burnt and unburnt habitats by large mammalian herbivores in a savanna-woodland ecosystem. Savanna-Woodland Fire Regimes Ecology Management and Conservation of African Protected Areas. Stellenbosch University, pp 304–351

Riginos C (2009) Grass competition suppresses savanna tree growth across multiple demographic stages. Ecology 90:335–340

Russell GG, Watson L, Koekemoer M, Smook L, Barker N, Anderson H, Dallwitz M (1990) others. Grasses of southern Africa. Number 58

Sagang LBT (2022) Monitoring Forest-Savanna Dynamics in the Guineo-Congolian Transition Area of the Centre Region of Cameroon. University of Yaoundey, pp 1-166

Sanou L, Savadogo P, Zida D, Thiombiano A (2022) Variation in soil seed bank and relationship with aboveground vegetation across microhabitats in a savanna-woodland of West Africa. Nordic J Bot. https://doi.org/10.1111/njb.03304

Scalon MC, Oliveras Menor I, Freitag R, Peixoto KS, Rifai SW, Marimon BS, Marimon BH, Malhi Y (2022) Contrasting strategies of nutrient demand and use between savanna and forest ecosystems in a Neotropical transition zone. Biogeosci Discuss 63:1–21

Scholes R, Archer S (1997) Interactions between woody plants and grasses in savannas. Annu Rev Ecol Syst 28:517–544

Sharma S, Singh G, Sharma M (2021) A Comprehensive Review and Analysis of Supervised-Learning and Soft Computing Techniques for Stress Diagnosis in Humans. Comput Biol Med 134:104450

Singh C (2022) Forest-savanna transitions Understanding adaptation and resilience of the tropical forest ecosystems using remote sensing. PhD thesis. Stockholm University

Staver AC, Levin SA (2012) Integrating theoretical climate and fire effects on savanna and forest systems. American Natur 180:211–224

Staver AC, Archibald S, Levin S (2011) Tree cover in sub-Saharan Africa: rainfall and fire constrain forest and savanna as alternative stable states. Ecology 92:1063–1072

Wang Z, Bao X, Wu T (2021) A parallel bioinspired algorithm for Chinese postman problem based on molecular computing. Comput Intell Neurosci. https://doi.org/10.1155/2021/8814947

Zhou Y, Singh J, Butnor JR, Coetsee C, Boucher PB, Case MF, Hockridge EG, Davies AB, Staver AC (2022) Limited increases in savanna carbon stocks over decades of fire suppression. Nature 603:1–5